Supporting Information

Mechanism and Kinetics of Methylating C_6–C_{12} Methylbenzenes with Methanol and Dimethyl Ether in H-MFI Zeolites

Mykela DeLuca, Pavlo Kravchenko, Alexander Hoffman, David Hibbitts*

Department of Chemical Engineering, University of Florida, Gainesville, 32611

*Corresponding author: hibbitts@che.ufl.edu

Table of Contents

S1. Details of MFI Restructuring and Reorientations

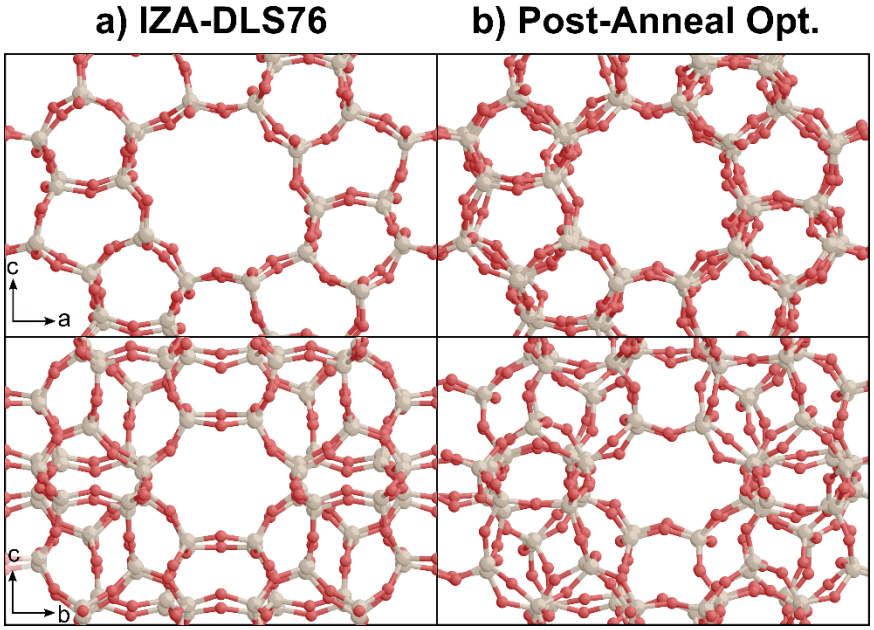

Figure S1. a) The initial, unoptimized silica form of MFI from the IZA database (IZA-DLS76) and **b)** the structure obtained after annealing and optimization using PBE-D. The post-anneal structure is 23 kJ mol^{-1} more stable than the directly optimized IZA-DLS76 structure.

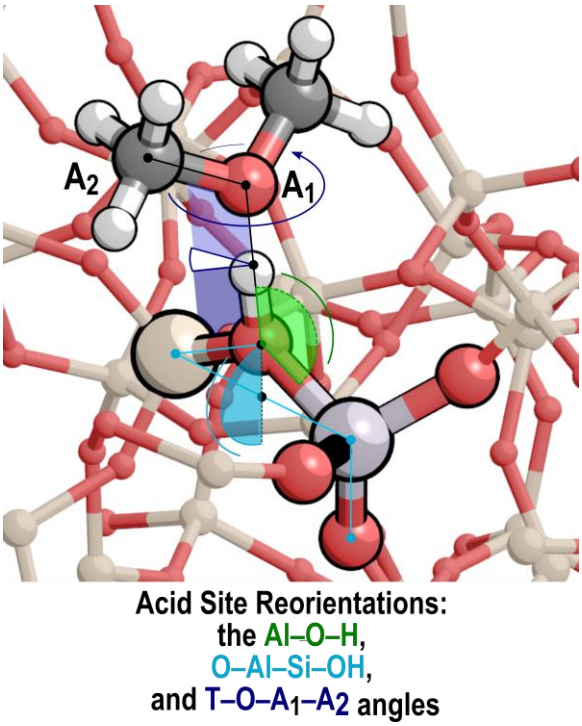

Figure S2. Three different acid site reorientations resulting from altering the Al–O_a–A_1 angle (green), O_t–Al–Si–O_a angle (cyan), and O_t–O_a–A_1–A_2 angle (blue).

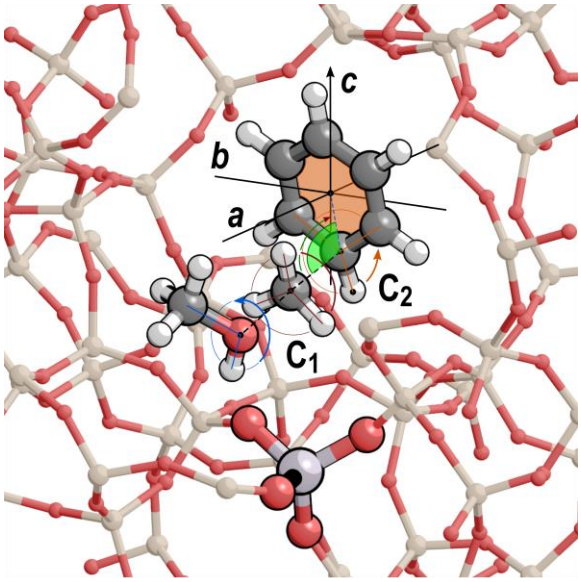

Figure S3. Internal reorientations of the concerted transition state where CH_3OH (blue), CH_3 (brown), and C_6H_6 can be rotated by altering the O_m–C_1–C_2 angle formed between the leaving group, the adding CH_3, and the ring (orange). The angle of the ring can be altered relative to the adding CH_3 group by altering the CH_3–ring angle (green).

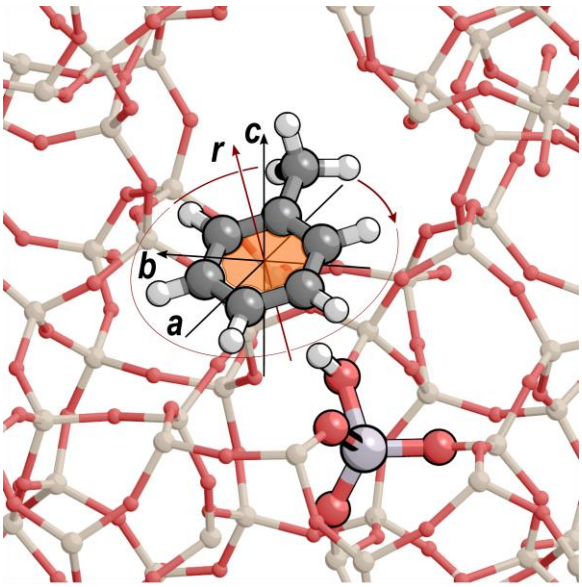

Figure S4. Spatial reorientations of toluene about the a, b, and c axes of the unit cell and the axis perpendicular to the center of the ring (red).

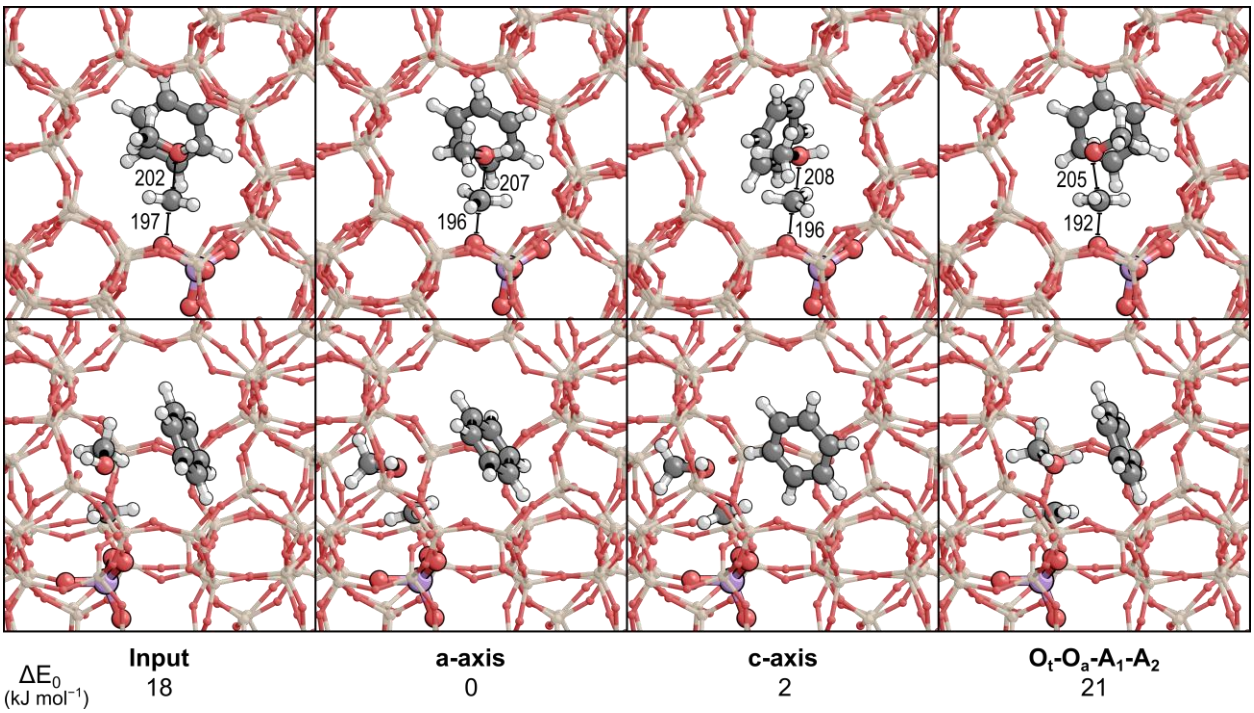

Figure S5. Different orientations of the benzene ring and surface methylation transition state during surface methylation near benzene. Bond distances between Al–O---CH_3 and CH_3---OCH_3H are shown in Angstroms. Views are shown down the straight (top) and sinusoidal (bottom) channels. Relative electronic energy values (kJ mol^{-1}) are reported relative to the most stable structure.

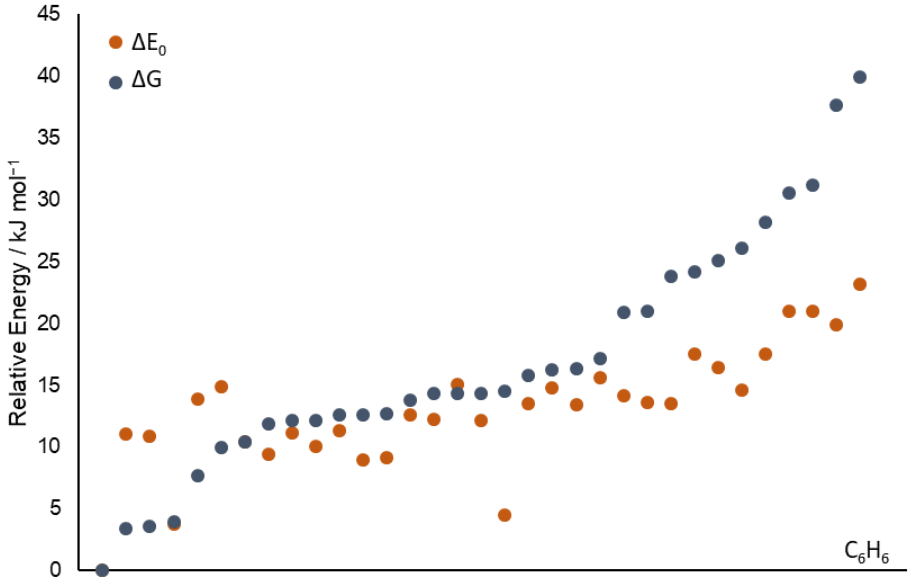

Figure S6. Energy (orange) and free energy (blue) of all optimized benzene re-orientations. Energies are relative to the state with the lowest free energy.

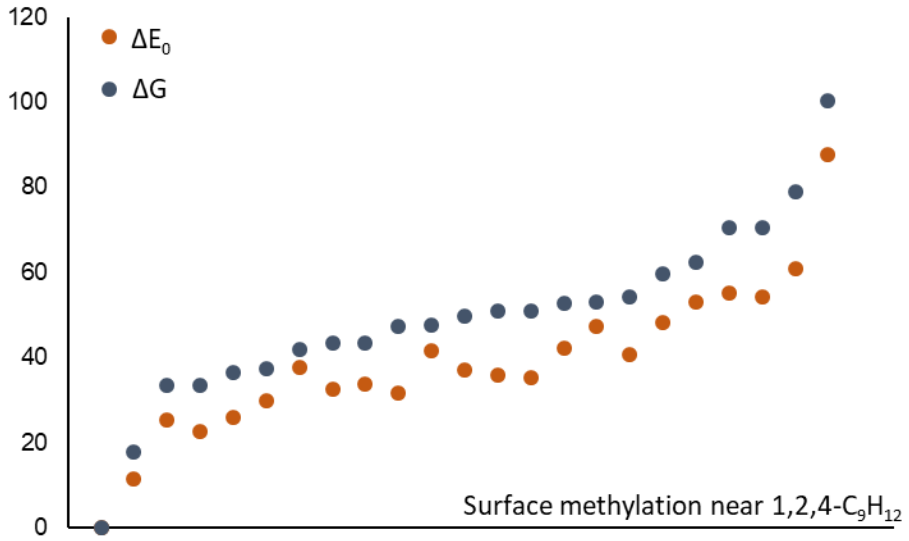

Figure S7. Energy (orange) and free energy (gray) of all optimized surface methylation near 1,2,4-trimethylbenzene transition states relative to the state with the lowest free energy.

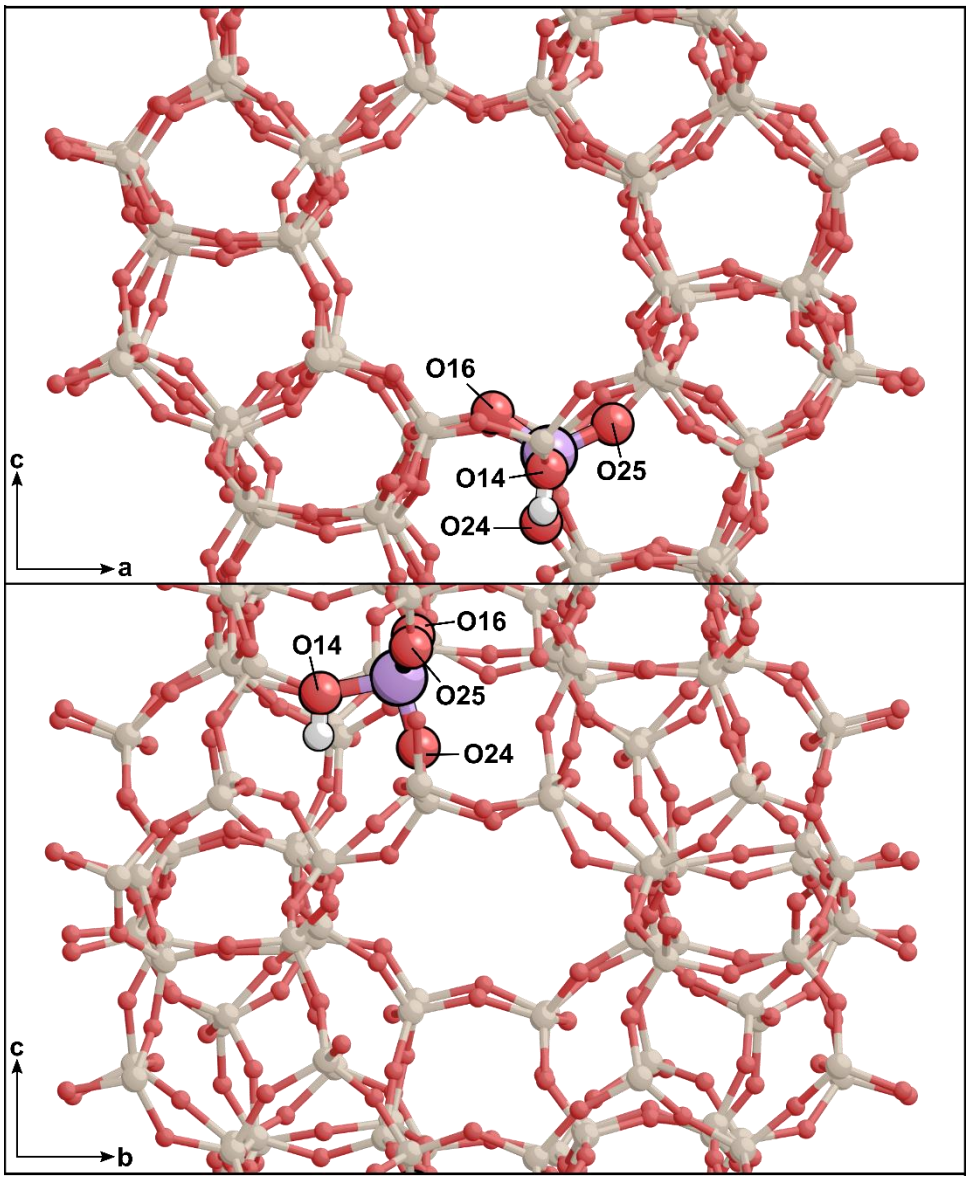

Figure S8. The location of each O-site at the T11 site in MFI along the straight (top) and sinusoidal (bottom) pores.

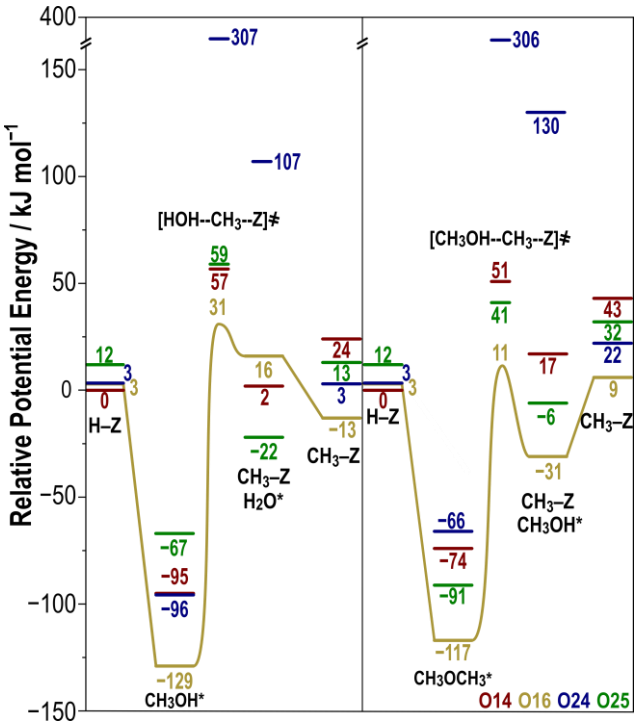

Figure S9. Reaction coordinate diagram of initial surface methylation energies (pre-reorientation) at O14 (red), O16 (yellow), O24 (blue), and O25 (green) with CH_3OH (left) and CH_3OCH_3 (right). The most favorable pathway determined by the lowest energy transition state occurs at O16 and is traced with lines. Potential energy values (kJ mol^{-1}) are relative to a proton on O14. Initial trends show energies increase as O16 < O14 < O25 < O24 with CH_3OH and O16 < O25 < O14 < O24 with CH_3OCH_3.

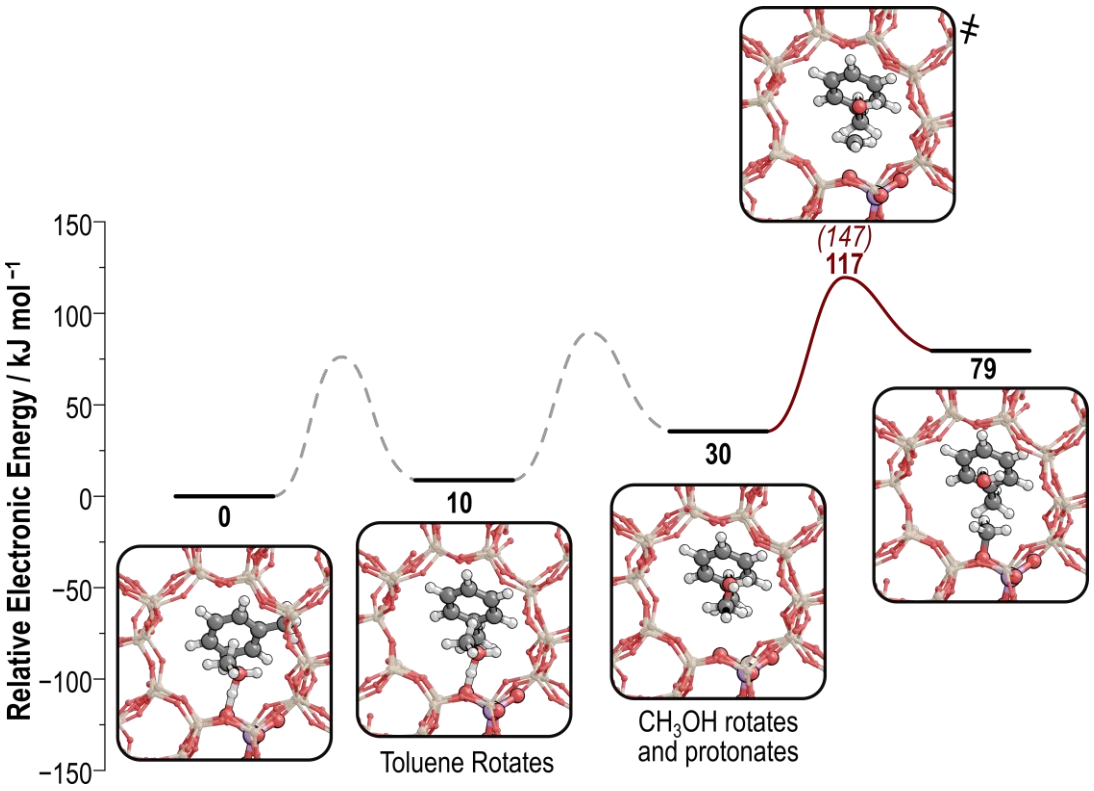

Figure S10. Electronic energies of toluene reorientation from the most stable reactant state to the orientation of the transition state. Reorientation barriers are estimated to be significantly less than the intrinsic barrier of surface methylation (147 kJ mol^{-1}), suggesting that they are kinetically irrelevant.

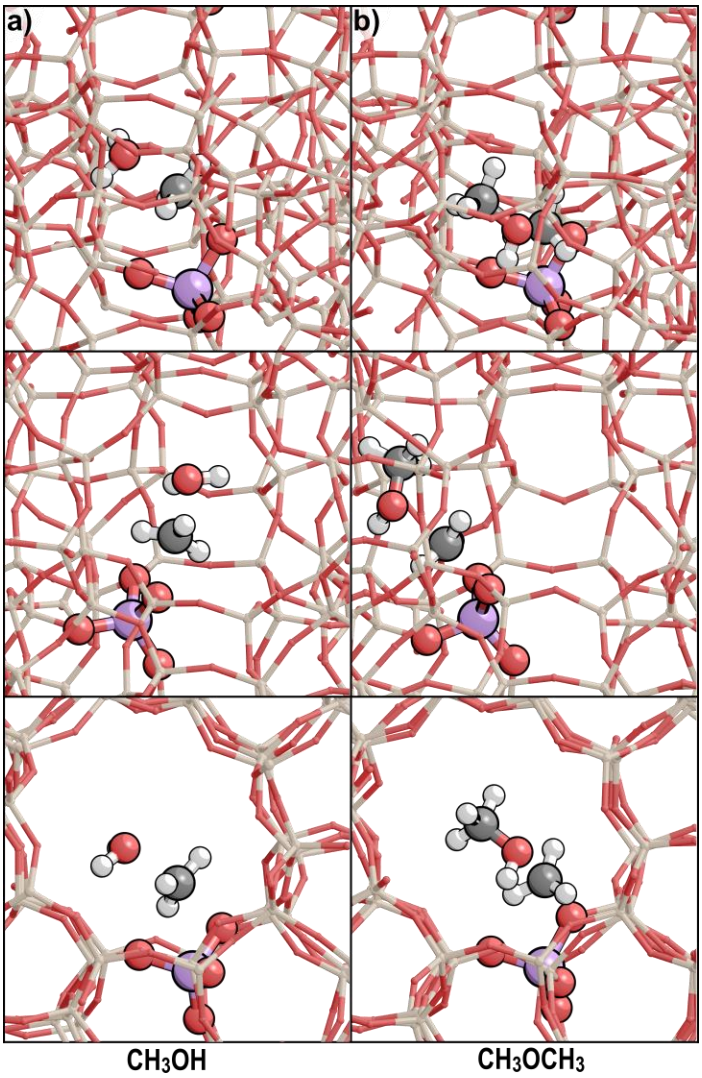

Figure S11. Extra views of surface methylation transition states without a spectating arene at O24 using **a)** CH_3OH and **b)** CH_3OCH_3.

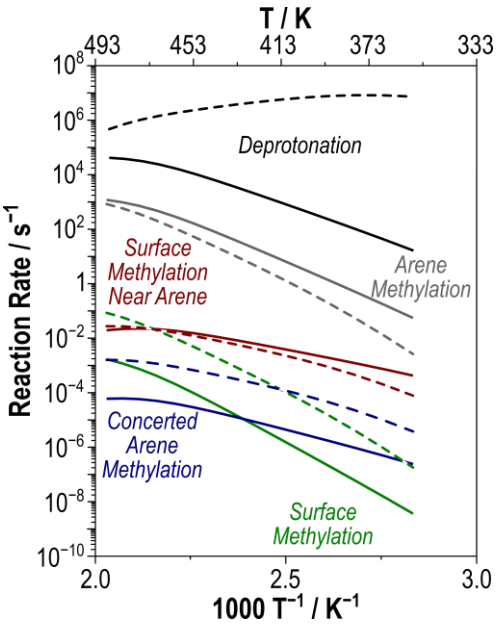

Figure S12. Rates of surface methylation (green), concerted methylation (blue), surface methylation near benzene (red), arene methylation (gray), and deprotonation of $C_7H_9^+$ to toluene with CH_3OH (solid) and CH_3OCH_3 (dashed). Rates are reported at 0.68 bar CH_3OR, 0.02 bar C_6H_6, 0.1% C_6H_6 conversion, from 353–493 K.

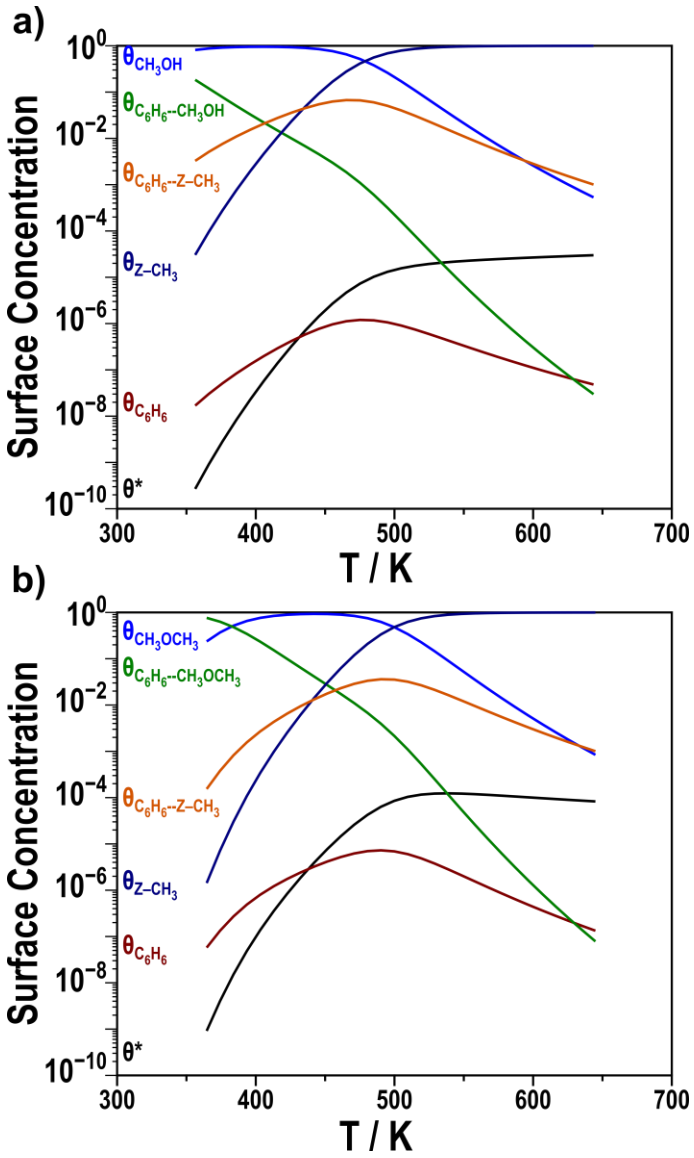

Figure S13. Evolution of surface species during benzene methylation with a) CH_3OH and b) CH_3OCH_3 from 353–653 K, 0.68 bar CH_3OH, 0.02 bar C_6H_6, 0.1% C_6H_6 conversion.

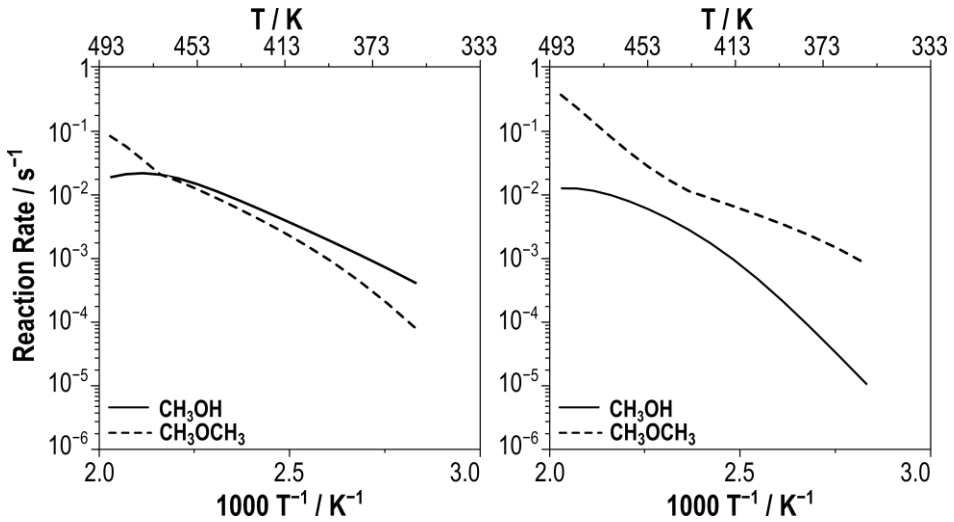

Figure S14. Overall rates of **a)** C_6H_6 and **b)** C_7H_8 methylation with CH_3OH (solid) and CH_3OCH_3 (dashed) between 353 K and 493 K, 0.68 bar CH_3OR, 0.02 C_6H_6 and 0.03 bar C_7H_8 0.1% conversion.

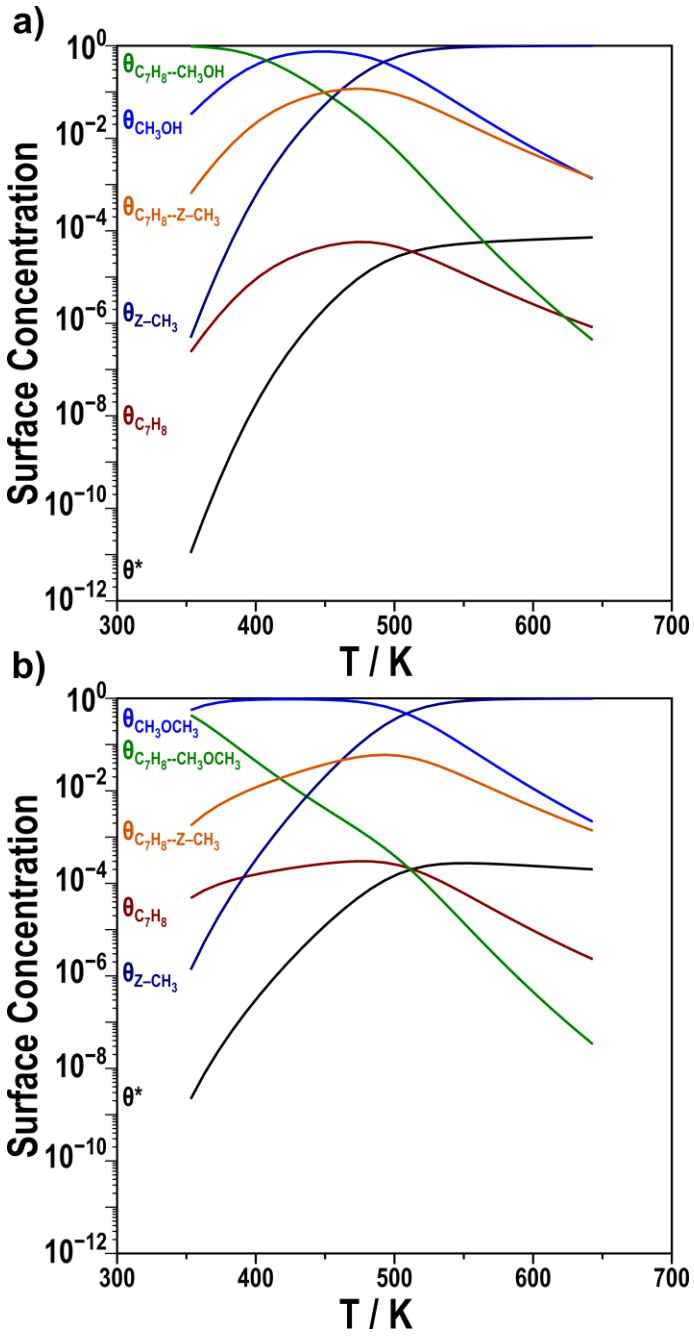

Figure S15. Evolution of surface species with a) CH_3OH and b) CH_3OCH_3 from 353–653 K, 0.68 bar CH_3OH, 0.03 bar C_7H_8, 0.1% C_7H_8 conversion.

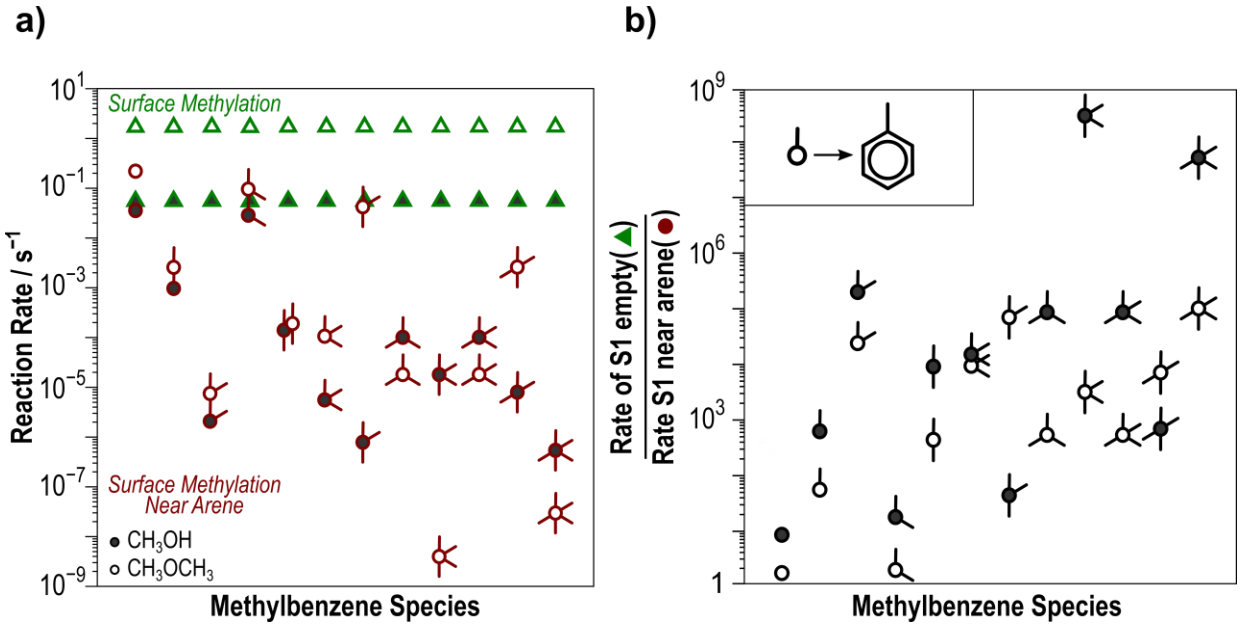

Figure S16. a) Maximum rate of surface methylation in an empty pore (green, triangles) and surface methylation with a spectating arene (red, circle) with CH_3OH (filled) and CH_3OCH_3 (empty), and **b)** ratio of the rate of surface methylation in an empty pore to the rate of surface methylation near arene with CH_3OH (filled) and CH_3OCH_3 (empty). Rates are reported at 0.04 bar C_xH_y, 0.08 bar CH_3OR, 10% aromatic conversion, and 623 K.

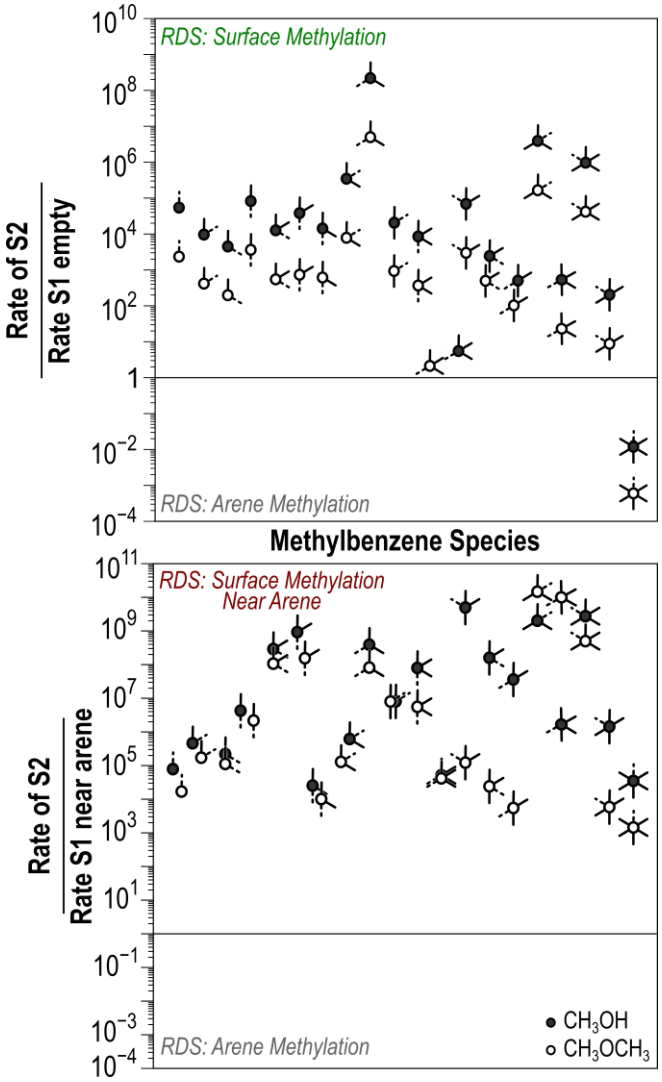

Figure S17. Ratio of ring methylation (second step of the sequential mechanism) maximum rate to rate of surface methylation (first step of the sequential mechanism) in an empty pore (top) and near a spectating arene (bottom) with CH_3OH (filled) and CH_3OCH_3 (empty). Values above 1 (horizontal gray line) signify that the surface methylation step is rate-determining while values below 1 signify arene methylation is rate-determining. Dashed lines represent the location of methyl-addition on the arene. Rates are reported at 0.04 bar C_xH_y, 0.08 bar CH_3OR, 10% aromatic conversion, and 623 K.

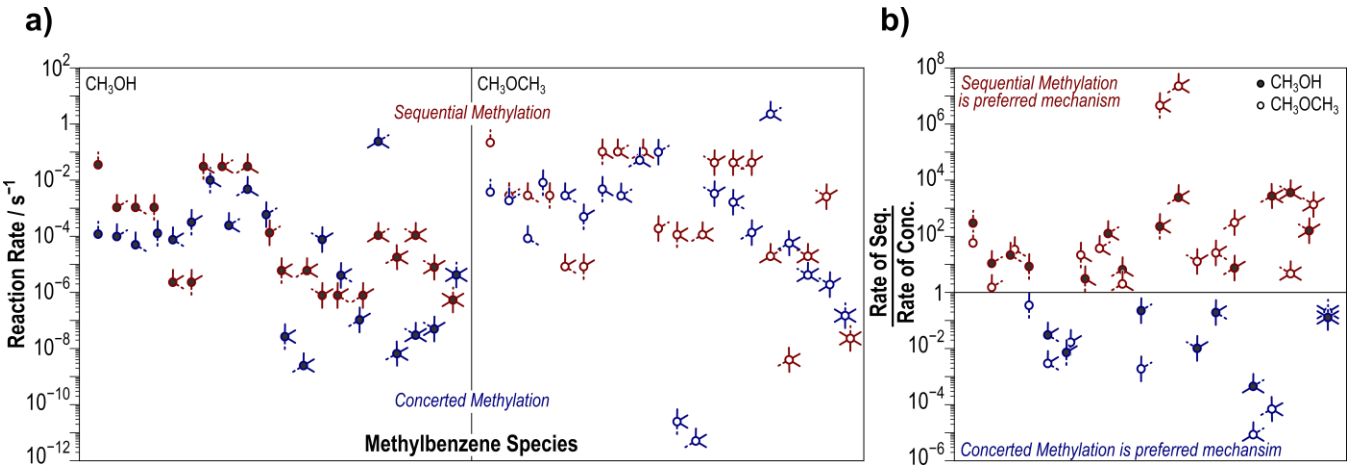

Figure S18. a) Rates of sequential (red) and concerted (blue) methylation with CH_3OH (filled) and CH_3OCH_3 (empty), and **b)** a ratio of concerted and sequential methylation rates. Rates are reported at 0.04 bar C_xH_y, 0.08 bar CH_3OR, 10% aromatic conversion, and 623 K.

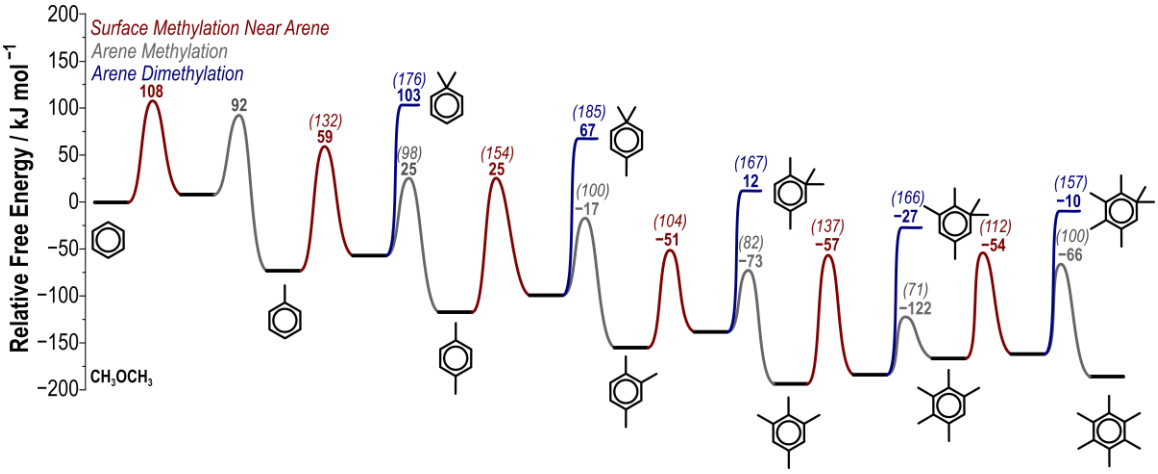

Figure S19. Reaction coordinate diagram showing sequential methylation barriers compared to geminal methylation barriers via methylation by CH_3–Z at 623K.

S2. Maximum Rate analysis of Arene Methylation Rates

Maximum rate analyses assert, one at a time, that a step is rate-determining and that all preceding steps are quasi-equilibrated. Maximum rate analysis permits identification of the rate-determining step (that with the lowest maximum rate in a pathway) and allows for direct comparison of experimentally obtained rates to those obtained from DFT. All rates are determined from transition state theory with activation entropies contributing to pre-exponential factors. Rate equations are derived based on the assumption of a single adsorption site that may contain isolated species (such as CH_3OR^* or $C_xH_y^*$) or complexes in which two species are adsorbed concurrently (such as C_xH_y--CH_3OR^*, which represents CH_3OH or CH_3OCH_3 and an arene present in the pore). All adsorption steps are assumed to be quasi-equilibrated and are represented by equilibrium constants as defined in Fig. 6.

Several potential site-occupying intermediates are considered in this analysis: CH_3OR*, C_xH_y*, CH_3–Z, C_xH_y--CH_3OR*, and C_xH_y--CH_3–Z where the final two intermediates represent arenes co-adsorbed with CH_3OR* or CH_3-Z (Fig. 6). A site-balance can then be described as:

$$\frac{[*]}{[L]} = \left(1 + K_{CH_3OR}(CH_3OR) + K_{C_xH_y}(C_xH_y) + K'_{S1}K'_{C_xH_y}(CH_3OR)(C_xH_y) + K_{S1}K_{CH_3OR}(K_{ROH})^{-1}\frac{(CH_3OR)}{(ROH)} + K'_{S1}K_{CH_3OR}K'_{C_xH_y}(K'_{ROH})^{-1}\frac{(CH_3OR)(C_xH_y)}{(ROH)}\right)^{-1} \quad (S1)$$

where species in parentheses indicate partial pressures and equilibrium constants are defined in Fig. 6 in the main text. The [*] term represents the concentration of unoccupied sites in the zeolite, and [L] represents all possible sites, regardless of their state (bare or occupied by guest species).

For the concerted methylation mechanism, there are three reaction steps: the adsorption of the methylating agent, CH_3OR, (K_{CH_3OR}, Eq. S2), the co-adsorption of the arene species to form a coordinated complex between the arene and methylating agent, $CH_3OR - C_xH_y^*$, ($K'_{C_xH_y}$, Eq. S3), and the methylation of the arene species (k, Eq. S4)

$$CH_3OR(g) + * \rightleftharpoons CH_3OR^* \qquad K_{CH_3OR} \qquad (S2)$$

$$C_xH_y(g) + CH_3OR^* \rightleftharpoons CH_3OR - C_xH_y^* \qquad K'_{C_xH_y} \qquad (S3)$$

$$CH_3OR - C_xH_y^* \rightarrow C_{x+1}H_{y+2}^* \qquad k_C \qquad (S4)$$

The product formation rate is simply the rate of depletion of the arene-methylating agent complex:

$$r = k_C\left[CH_3OR - C_xH_y^*\right] \qquad (S5)$$

The rate can be described in terms of partial pressures of each reactant species by combining with Eq. S2–S3 with Eq. S5:

$$r = K_{CH_3OR}K'_{C_xH_y}k_C(C_xH_y)(CH_3OR)[*] \qquad (S6)$$

Normalizing by the number of sites [L] yields a turnover rate for concerted methylation, yielding a general form of the rate equation for concerted arene methylation:

$$\frac{r}{L} = k_cK'_{C_xH_y}K_{CH_3OR}(CH_3OR)(C_xH_y)\left(\frac{[*]}{[L]}\right) \qquad (S7)$$

This form of the equation assumes no prior methylation to form the arene occurs and that the arene simply adsorbs prior to reaction.

In the sequential mechanism, there are four reaction steps: adsorption of the methylating agent (Eq. S8), methylation of the acid site (Eq. S9), adsorption of the arene species (Eq. S10), and methylation of the arene (Eq. S11). Several rate equations can be derived depending on which reaction step is rate determining. If surface methylation is rate determining, i.e.:

$$CH_3OR\ (g)\ + * \rightleftharpoons CH_3OR^* \qquad K_{CH_3OR} \qquad (S8)$$

$$CH_3OR^* \rightarrow CH_3^* + H_2O\ (g) \qquad k_{S1} \qquad (S9)$$

$$CH_3^* + C_xH_y(g) \rightleftharpoons CH_3 - C_xH_y^* \qquad Kinetically\ Irrelevant \qquad (S10)$$

$$CH_3 - C_xH_y^* \leftrightarrow C_{x+1}H_{y+2}^* \qquad Kinetically\ Irrelevant \qquad (S11)$$

where steps labeled "kinetically irrelevant" need not be considered in kinetic analysis as they occur after the rate-determining step. In this case, the arene methylation rate is simply dependent on the concentration of adsorbed CH_3OH or CH_3OCH_3:

$$r = k_{S1}[CH_3OR^*] \tag{S12}$$

When expressed in terms of reactant pressures and normalized by the number of sites, the turnover rate becomes:

$$\frac{r}{L} = k_{S1}K_{CH_3OR}(CH_3OR)\left(\frac{[*]}{[L]}\right) \tag{S13}$$

Surface methylation in the sequential pathway can also occur in the presence of a co-adsorbed arene species. Arene adsorption in this pathway occurs after the methylating agent adsorbs but before the surface methoxy group is formed. If surface methylation in the presence of an arene species is the rate determining step (RDS), the mechanism becomes:

$$CH_3OR\ (g) + * \rightleftharpoons CH_3OR^* \qquad K_{CH_3OR} \tag{S14}$$

$$C_xH_y(g) + CH_3OR^* \rightleftharpoons CH_3OR - C_xH_y^* \qquad K'_{C_xH_y} \tag{S15}$$

$$CH_3OR - C_xH_y^* \rightarrow\ CH_3 - C_xH_y^* + H_2O\ (g) \qquad k'_{S1} \tag{S16}$$

$$CH_3 - C_xH_y^* \leftrightarrow C_{x+1}H_{y+2}^* \qquad Kinetically\ Irrelevant \tag{S17}$$

Then the rate becomes dependent on the concentration of the complex formed by co-adsorbed arene and CH_3OR:

$$r = k'_{S1}[CH_3OR - C_xH_y^*\ ] \tag{S18}$$

And in terms of reactant pressures the turnover rate is:

$$\frac{r}{L} = k'_{S1}K'_{C_xH_y}K_{CH_3OR}(CH_3OR)\big(C_xH_y\big)\left(\frac{[*]}{[L]}\right) \tag{S19}$$

Finally, if arene methylation is the rate determining step in the sequential mechanism, then the coefficients for the mechanism become

$$CH_3OR\ (g) + * \rightleftharpoons CH_3OR^* \qquad K_{CH_3OR} \tag{S20}$$

$$C_xH_y(g) + CH_3OR^* \rightleftharpoons CH_3OR - C_xH_y^* \qquad K'_{C_xH_y} \tag{S21}$$

$$CH_3OR - C_xH_y^* \rightleftharpoons CH_3 - C_xH_y^* + H_2O\ (g) \qquad K_1{}' \tag{S22}$$

$$CH_3 - C_xH_y^* \rightarrow C_{x+1}H_{y+2}^* \qquad k_{S2} \tag{S23}$$

The rate, therefore, becomes dependent on the coverage of adsorbed arene near surface methoxy species.

$$r = k_{S2}\big[CH_3 - C_xH_y^*\big] \tag{S24}$$

$$r = k_{S2}K_{CH_3OR}(K_{ROH})^{-1}K'_{C_xH_y}K'_1\big(C_xH_y\big)(CH_3OR)(HOR)^{-1}[*] \tag{S25}$$

Where K_{ROH} represents the desorption of water when CH_3—C_xH_y is present in the pore. When the rate is normalized per site, the turnover rate becomes:

$$\frac{r}{L} = k_{S2} K_{CH_3OR} (K_{ROH})^{-1} K''_{C_xH_y} K_1 (C_xH_y)(CH_3OR)(ROH)^{-1} \left(\frac{[*]}{[L]}\right) \quad \text{(S26)}$$

The concentration of each species can be expressed in terms of conversion, as shown in Table S1.

Table S1. Mole balance expressions for each species expressed in terms of pressure and conversion.

Species	Initial	Change	Remaining
C_xH_y	$P_{C_xH_y,0}$	$-P_{C_xH_y,0}X$	$P_{C_xH_y,0}(1-X)$
CH_3OR	$\frac{P_{CH_3OR,0}}{P_{C_xH_y,0}} P_{C_xH_y,0}$	$-P_{C_xH_y,0}X$	$P_{C_xH_y,0}\left(\frac{P_{CH_3OR}}{P_{C_xH_y}} - X\right)$
ROH	0	$-P_{C_xH_y,0}X$	$-P_{C_xH_y,0}X$

Substituting into the expressions for methylation rate for each mechanism and RDS:

$$\frac{[*]}{[L]} = \left(1 + K_{CH_3OR} P_{C_xH_y}\left(\frac{P_{CH_3OR}}{P_{C_xH_y}} - X\right) + K_{C_xH_y} P_{C_xH_y}(1-X) + K_{CH_3OR} K'_{C_6H_6} P^2_{C_xH_y,0}(1-X)\left(\frac{P_{CH_3OR}}{P_{C_xH_y}} - X\right) + K_{CH_3OR} K_1 (K_{ROH})^{-1} P_{C_xH_y,0} \frac{(1-X)}{X} + K_{CH_3OR} K_{C_6H_6} K'_1 (K_{ROH})^{-1} P_{C_xH_y,0} \frac{(1-X)\left(\frac{P_{CH_3OR}}{P_{C_xH_y}} - X\right)}{X}\right)^{-1} \quad \text{(S27)}$$

The rate equations for each possible RDS can also be expressed in terms of conversion. The rate equations when surface methylation in the absence of co-adsorbed arene is the RDS becomes

$$r = k_{S1} K_{CH_3OR} P_{C_xH_y,0}(1-X) \quad \text{(S28)}$$

When arene adsorption occurs before surface methylation, but surface methylation is still the RDS, the rate equations becomes:

$$r = k'_{S1} K_{CH_3OR} K'_{C_6H_6} P_{C_xH_y,0}\left(\frac{P_{C_xH_y,0}}{P_{CH_3OR,0}} - X\right) \quad \text{(S29)}$$

However, if arene methylation is the RDS, then the rate equation based on conversion becomes:

$$r = k_{S2} K_{CH_3OR} K'_{S1} K'_{C_6H_6} (K'_{ROH})^{-1} P_{C_xH_y,0} \frac{(1-X)\left(\frac{P_{CH_3OR,0}}{P_{C_xH_y,0}} - X\right)}{X} \quad \text{(S30)}$$

Finally, if the concerted pathway prevails, then the rate equation follows as:

$$r = k_C K_{CH_3OR} K'_{C_6H_6} P_{C_xH_y,0}(1-X)\left(\frac{P_{CH_3OR,0}}{P_{C_xH_y,0}} - X\right) \quad \text{(S31)}$$

S3. Trimethyloxonium Formation

There are two mechanisms through which trimethyloxonium (TMO) species can form: a two-step mechanism in which the surface is first methylated by CH_3OCH_3 and a second CH_3OCH_3 is subsequently methylated by CH_3–Z (Figure S15a–b). Or a one-step mechanism in which two CH_3OCH_3 directly react to form TMO (Figure S15c–d). Once TMO species are formed, it is

possible that they will contribute to methylation of the zeolite surface or the arene. We have employed maximum rate analyses to compare the rates of these TMO formation mechanisms and evaluate their contributions to benzene methylation.

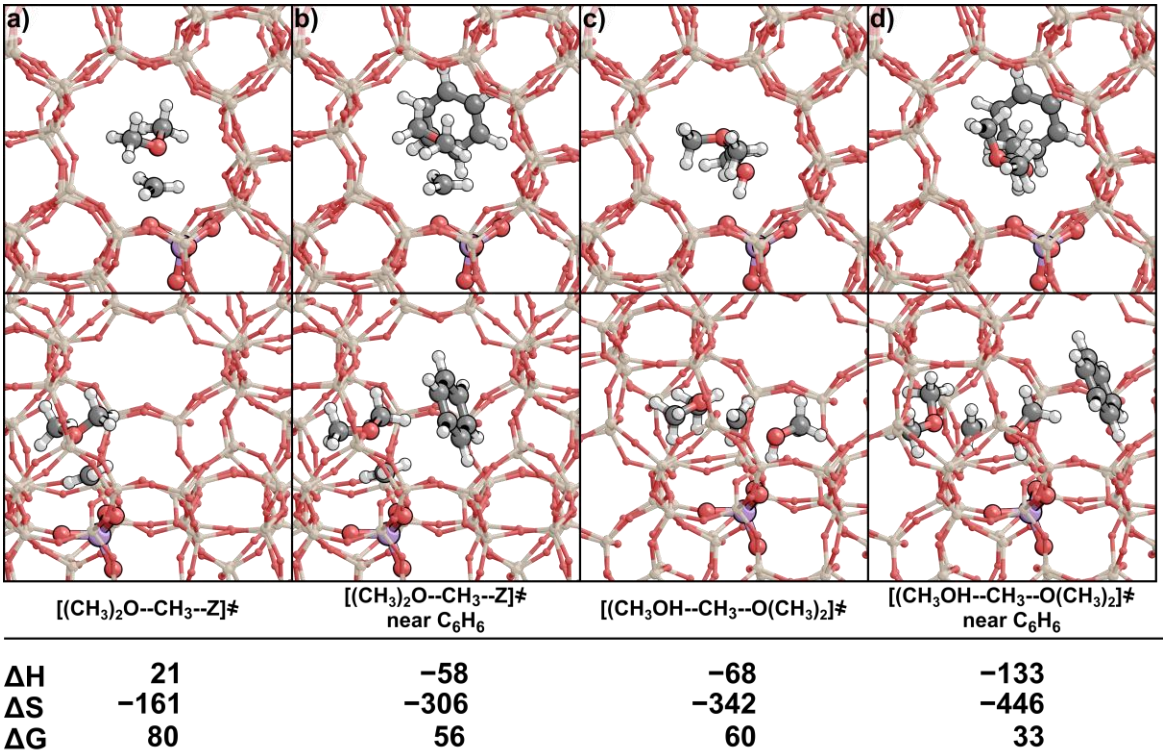

Figure S20. The transition state structure of trimethyloxonium formation from methylation by CH_3–Z in a) in an empty pore and b) with a spectating benzene and via reaction of two CH_3OCH_3 in a) an empty pore and b) with spectating benzene. Views are presented down the straight (top) and sinusoidal (bottom) channels. Enthalpy (kJ mol^{-1}), entropy (J mol^{-1} K^{-1}), and free energy (kJ mol^{-1}) are reported at 373 K and 1 bar.

There are 3 possible rate-determining steps in the one-step TMO formation mechanism that we will analyze with maximum rate analysis. The first is formation of TMO from the reaction of two CH_3OCH_3 molecules

$$CH_3OCH_3(g) + * \rightarrow CH_3OCH_3^* \qquad K_{CH_3OCH_3} \qquad \text{(S32)}$$

$$CH_3OCH_3^* + CH_3OCH_3(g) \rightarrow CH_3OCH_3 \cdots CH_3OCH_3^* \qquad K''''_{CH_3OCH_3} \qquad \text{(S33)}$$

$$CH_3OCH_3 \cdots CH_3OCH_3^* \rightarrow TMO^+ \cdots CH_3OH^* \qquad k_{TMO_C} \text{ or } K_{TMO_C} \qquad \text{(S34)}$$

$$TMO^+ \cdots CH_3OH^* \rightarrow TMO^{+*} + CH_3OH(g) \qquad \left(K''''_{CH_3OH}\right)^{-1} \qquad \text{(S35)}$$

The rate of this reaction can be expressed by

$$r = K_{CH_3OCH_3} K''''_{CH_3OCH_3} k_{TMO_C} (CH_3OCH_3)^2 \frac{[*]}{L} \qquad \text{(S36)}$$

After the formation of TMO, it can either methylate the zeolite surface

$$TMO^{+*} \rightarrow CH_3 - Z \cdots CH_3OH \qquad k_{TMO_{SM}} \qquad \text{(S37)}$$

Which has rate

$$r = K_{CH_3OCH_3} K'''''_{CH_3OCH_3} K_{TMO_C} \left(K''''_{CH_3OH}\right)^{-1} k_{TMO_{SM}} \frac{(CH_3OCH_3)^2}{(CH_3OH)} \frac{[*]}{L} \qquad \text{(S38)}$$

Or it can methylate a benzene ring

$$TMO^{+*} + C_6H_6(g) \rightarrow TMO^{+} \cdots C_6H_6^* \qquad K'''_{C_6H_6} \qquad \text{(S39)}$$

$$TMO^{+} \cdots C_6H_6^* \rightarrow CH_3OCH_3 \cdots C_7H_9^* \qquad k_{TMO_m} \text{ or } K_{TMO_m} \qquad \text{(S40)}$$

Leading to a rate of

$$r = K_{CH_3OCH_3} K'''''_{CH_3OCH_3} K_{TMO_C} \left(K''''_{CH_3OH}\right)^{-1} K'''_{C_6H_6} k_{TMO_m} \frac{(CH_3OCH_3)^2(C_6H_6)}{(CH_3OH)} \frac{[*]}{L} \qquad \text{(S41)}$$

Alternatively, the elementary steps S32–S37 can occur with spectating benzene changing equation S36 to

$$r = K_{CH_3OCH_3} K'''''_{CH_3OCH_3} K'''_{C_6H_6} k'_{TMO_C} (CH_3OCH_3)^2 (C_6H_6) \frac{[*]}{L} \qquad \text{(S42)}$$

And equation S38 becomes

$$r = K_{CH_3OCH_3} K'''''_{CH_3OCH_3} K'''_{C_6H_6} K_{TMO_C} \left(K''''_{CH_3OH}\right)^{-1} k_{TMO_{SM}} \frac{(CH_3OCH_3)^2(C_6H_6)}{(CH_3OH)} \frac{[*]}{L} \qquad \text{(S43)}$$

The two-step TMO formation mechanism also has three possible rate-determining steps. The first is formation of CH_3–Z species, similar the previously describe sequential arene methylation mechanism

$$CH_3OCH_3(g) + * \rightarrow CH_3OCH_3^* \qquad K_{CH_3OCH_3} \qquad \text{(S44)}$$

$$CH_3OCH_3^* \rightarrow Z - CH_3 \cdots CH_3OH^* \qquad k_{s1} \text{ or } K_{S1} \qquad \text{(S45)}$$

$$Z - CH_3 \cdots CH_3OH^* \rightarrow Z - CH_3 + CH_3OH(g) \qquad \left(K''_{CH_3OH}\right)^{-1} \qquad \text{(S46)}$$

This reaction occurs with a rate of

$$r = K_{CH_3OCH_3} k (CH_3OCH_3) \frac{[*]}{L} \qquad \text{(S47)}$$

Once the CH_3–Z species is formed, it can react with a second CH_3OCH_3 molecule to form TMO

$$Z - CH_3 + CH_3OCH_3(g) \rightarrow Z - CH_3 \cdots CH_3OCH_3^* \qquad K''''_{CH_3OCH_3} \qquad \text{(S48)}$$

$$Z - CH_3 \cdots CH_3OCH_3^* \rightarrow TMO^{+*} \qquad k_{TMO_s} \text{ or } K_{TMO_s} \qquad \text{(S49)}$$

$$r = K_{CH_3OCH_3} K_{S1} \left(K''_{CH_3OH}\right)^{-1} K''''_{CH_3OCH_3} k_{TMO_s} \frac{(CH_3OCH_3)^2}{(CH_3OH)} \frac{[*]}{L} \qquad \text{(S50)}$$

Finally, the TMO can methylate benzene to form toluene

$$TMO^{+*} + C_6H_6(g) \rightarrow TMO^{+} \cdots C_6H_6^* \qquad K'''_{C_6H_6} \qquad \text{(S51)}$$

$$TMO^{+} \cdots C_6H_6^{*} \rightarrow CH_3OCH_3 \cdots C_7H_9^{*} \qquad k_{TMO_m} \text{ or } K_{TMO_m} \qquad \text{(S52)}$$

$$r = K_{CH_3OCH_3} K_{S1} \left(K''_{CH_3OH}\right)^{-1} K''''_{CH_3OCH_3} K_{TMO_s} K'''_{C_6H_6} k_{TMO_m} \frac{(CH_3OCH_3)^2(C_6H_6)}{(CH_3OH)} \frac{[*]}{L} \qquad \text{(S53)}$$

Similar to the one-step mechanism, the first two rate-determining steps can also occur with spectating benzene changing the rate equation of Eq. S47 to

$$r = K_{CH_3OCH_3} K''_{C_6H_6} k'_{S1} (CH_3OCH_3)(C_6H_6) \frac{[*]}{L} \qquad \text{(S54)}$$

And Eq. S50 becomes

$$r = K_{CH_3OCH_3} K''_{C_6H_6} K'_{S1} \left(K'''_{CH_3OH}\right)^{-1} K''''_{CH_3OCH_3} k'_{TMO_s} \frac{(CH_3OCH_3)^2(C_6H_6)}{(CH_3OH)} \frac{[*]}{L} \qquad \text{(S55)}$$

Using these rate equations, we can evaluate the rates of these reaction pathways and compare them to the arene methylation pathways discussed in Section S2.

Section 3 of the manuscript demonstrated that surface methylation with spectating benzene occurs with higher rates than surface methylation in an empty pore; therefore, only surface methylation with spectating benzene is considered in this discussion. Rates of the one-step mechanism are lower than surface methylation with spectating benzene, suggesting that this one-step TMO formation mechanism is not kinetically relevant. Similar to surface methylation, the intrinsic barrier of TMO formation via methylation of CH_3OCH_3 by CH_3–Z is lowered by 10 kJ mol^{-1} (from 82 kJ mol^{-1} to 72 kJ mol^{-1}) and thus TMO formation via the sequential mechanism occurs with higher rates when benzene is present (Figure S16). At temperatures below 423 K, the reaction of CH_3–Z species with CH_3OCH_3 occurs at a higher rate than reaction of CH_3–Z with C_6H_6 to form toluene; therefore, at low temperatures we predict methylation by TMO is contributing to the formation of C_7H_8 species. However, the rate of C_6H_6 methylation by CH_3–Z, the formation of TMO by CH_3OCH_3 reaction with CH_3–Z, and C_6H_6 methylation by TMO are all facile compared to the formation of CH_3–Z species indicating that the overall rate of sequential methylation is not significantly impacted when considering this additional sequential TMO route.

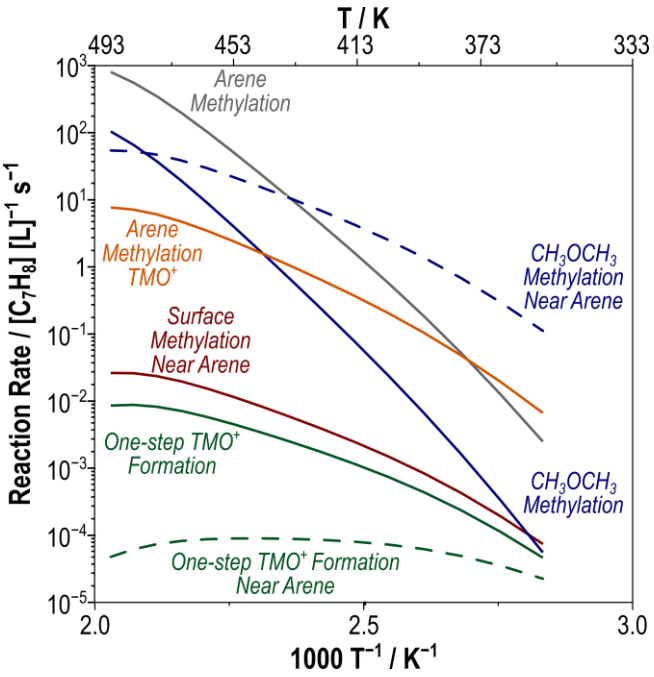

Figure S21. Rates of surface methylation (CH_3–Z formation) with CH_3OCH_3 and spectating benzene (red), reaction of two CH_3OCH_3 to form TMO in an empty pore (green, solid) and with spectating benzene (green, dashed), methylation of CH_3OCH_3 with Z–CH_3 in an empty pore (blue, solid) and with spectating benzene (blue, dashed), arene methylation with CH_3–Z (gray), and arene methylation with TMO (orange). Rates are shown at 373 K, 0.02 bar C_6H_6, 0.68 bar CH_3OCH_3, and 0.1% aromatic conversion.

S4. Reaction and Transition State Energies

Table S2. Adsorption enthalpy and entropy of methylbenzene species

Species	ΔH_{ads}[a] kJ mol^{-1}	ΔS_{ads} J mol^{-1} K^{-1}
Benzene	-66.8	-123.2
Toluene	-92.9	-155.8
ortho-xylene	-90.7	-166.7
meta-xylene	-94.6	-183.9
para-xylene	-86.8	-161.6
1,2,3-trimethylbenzene	-87.2	-183.7
1,2,4-trimethylbenzene	-96.8	-204.1
1,3,5-trimethylbenzene	-97.4	-157.5
1,2,3,4-tetramethylbenzene	-101.2	-195.2
1,2,3,5-tetramethylbeznene	-80.8	-185.6
1,2,4,5-tetramethylbenzene	-71.8	-208.6
Pentamethylbenzene	-44.5	-225.3
Hexamethylbenzene	-43.5	-236.1

[a] ΔH_{ads} values are reported at 473 K

Table S3. Reaction and activation barriers of surface methylation.

Spectating Species	Methylation Agent							
	CH_3OH				CH_3OCH_3			
	ΔH_{act}[a] kJ mol^{-1}	ΔS_{act} J mol^{-1} K^{-1}	ΔH_{rxn}[a] kJ mol^{-1}	ΔS_{rxn} J mol^{-1} K^{-1}	ΔH_{act}[a] kJ mol^{-1}	ΔS_{act} J mol^{-1} K^{-1}	ΔH_{rxn}[a] kJ mol^{-1}	ΔS_{rxn} J mol^{-1} K^{-1}
Empty	144.1	1.1	88.9	47.8	124.7	-10.8	82.4	23.0
Benzene	102.3	-7.6	68.8	21.8	118.2	11.6	83.3	37.8
Toluene	117.5	-18.0	85.4	18.6	112.2	-5.3	98.9	13.0
ortho-xylene	130.7	-32.5	103.3	10.6	134.1	-16.0	123.9	-1.1
meta-xylene	114.8	-11.5	82.5	30.4	129.4	18.1	107.1	35.7
para-xylene	135.7	-1.3	105.1	27.4	148.1	8.3	148.7	15.2
1,2,3-tri	114.9	-5.4	86.1	32.9	124.4	11.9	108.5	21.3
1,2,4-tri	126.6	-14.9	96.4	24.1	124.8	4.0	95.2	34.0
1,3,5-tri	110.1	-22.4	82.4	22.4	135.0	3.9	106.4	29.2
1,2,3,4-tetra	104.9	-22.8	111.7	21.1	140.2	-17.8	78.8	38.6
1,2,3,5-tetra	105.3	1.1	79.2	28.9	120.0	-13.4	88.7	5.9
1,2,4,5-tetra	105.1	-3.6	87.1	39.8	129.6	31.5	122.9	20.4
Penta	93.5	-10.3	66.8	21.6	109.8	-27.3	55.1	13.5

[a]ΔH_{act} and ΔH_{rxn} are reported at 473 K

Table S4. Activation Energy of surface methylation transition states.

Reactants	Products	ΔH_{act}[a] kJ mol^{-1}	ΔS_{act}[a] J mol^{-1} K^{-1}
Benzene	Toluene	71.4	-20.8
Toluene	*Ortho*	75.0	-25.1
Toluene	*Meta*	83.3	-20.5
Toluene	*Para*	71.0	-17.3
Ortho	1,2,3-tri	70.5	-18.9
Ortho	1,2,4-tri	66.3	-21.4
Meta	1,3,5-tri	64.4	-38.7
Meta	1,2,3-tri	62.2	-27.3
Meta	1,2,4-tri	33.3	-22.3
Para	1,2,4-tri	74.5	-12.2
1,2,3-tri	1,2,3,4-tetra	52.1	-19.3
1,2,3-tri	1,2,3,5-tetra	76.1	-20.6
1,2,4-tri	1,2,3,4-tetra	62.6	-4.4
1,2,4-tri	1,2,3,5-tetra	69.4	-6.1
1,2,4-tri	1,2,4,5-tetra	62.9	-20.7
1,3,5-tri	1,2,3,5-tetra	55.3	-26.9
1,2,3,4-tetra	Penta	61.5	-18.0
1,2,3,5-tetra	Penta	56.1	-8.6
1,2,4,5-tetra	Penta	37.5	-14.7
penta	Hexa	87.6	-12.7

[a]ΔH_{act} values are reported at 473 K

Table S5. Activation enthalpies and energies of concerted methylation.

Reactants	Products	Methylation Agent			
		CH_3OH		CH_3OCH_3	
		ΔH_{act}[a] kJ mol^{-1}	ΔS_{act} J mol^{-1} K^{-1}	ΔH_{act}[a] kJ mol^{-1}	ΔS_{act} J mol^{-1} K^{-1}
Benzene	Toluene	119.9	-20.0	120.0	-8.4
Toluene	*Ortho*	127.2	-20.9	118.6	-1.0
Toluene	*Meta*	133.7	-17.7	121.7	-14.4
Toluene	*Para*	130.0	-16.5	102.5	-9.7
Ortho	1,2,3-tri	131.7	-12.9	126.7	7.4
Ortho	1,2,4-tri	122.8	-18.7	125.5	-3.2
Meta	1,3,5-tri	112.7	-19.7	122.5	-5.6
Meta	1,2,3-tri	130.0	-25.1	119.5	-11.6
Meta	1,2,4-tri	121.7	-18.0	120.9	5.3
Para	1,2,4-tri	108.9	-21.2	126.2	19.2
1,2,3-tri	1,2,3,4-tetra	136.7	-11.9	143.9	-7.1
1,2,3-tri	1,2,3,5-tetra	140.5	-7.6	151.6	-2.2
1,2,4-tri	1,2,3,4-tetra	118.8	1.5	118.5	-16.3
1,2,4-tri	1,2,3,5-tetra	126.8	3.7	133.9	-4.0
1,2,4-tri	1,2,4,5-tetra	138.8	-3.5	140.2	-10.9
1,3,5-tri	1,2,3,5-tetra	109.9	-24.0	102.3	-10.7
1,2,3,4-tetra	Penta	139.3	-29.6	165.7	2.4
1,2,3,5-tetra	Penta	146.8	0.1	119.6	-22.0
1,2,4,5-tetra	Penta	116.5	-19.2	142.0	5.9
Penta	Hexa	83.5	-9.6	101.1	-28.1

[a] ΔH_{act} values are reported at 473 K

S5. Details of Thermochemical Properties of Frequency Calculations

Frequency calculations were performed on all optimization and Dimer calculations. Frequency calculations are normal mode analyses and are used to determine zero-point vibrational energy (ZPVE), vibrational enthalpy (Hvib), and vibrational free energy (Gvib) for adsorbed species to calculate enthalpy (H):

$$H = E_0 + ZPVE + H_{vib} \quad \text{(S56)}$$

and free energies (G):

$$G = E_0 + ZPVE + G_{vib} \quad \text{(S57)}$$

Translational and rotational enthalpies and free energies are also calculated for gas phase species to determine gas phase enthalpy:

$$H = E_0 + ZPVE + H_{vib} + H_{rot} + H_{trans} \quad \text{(S58)}$$

and gas phase free energies:

$$G = E_0 + ZPVE + G_{vib} + G_{rot} + G_{trans} \quad \text{(S59)}$$

S6. Most favorable orientations of reactant, product, and transition states

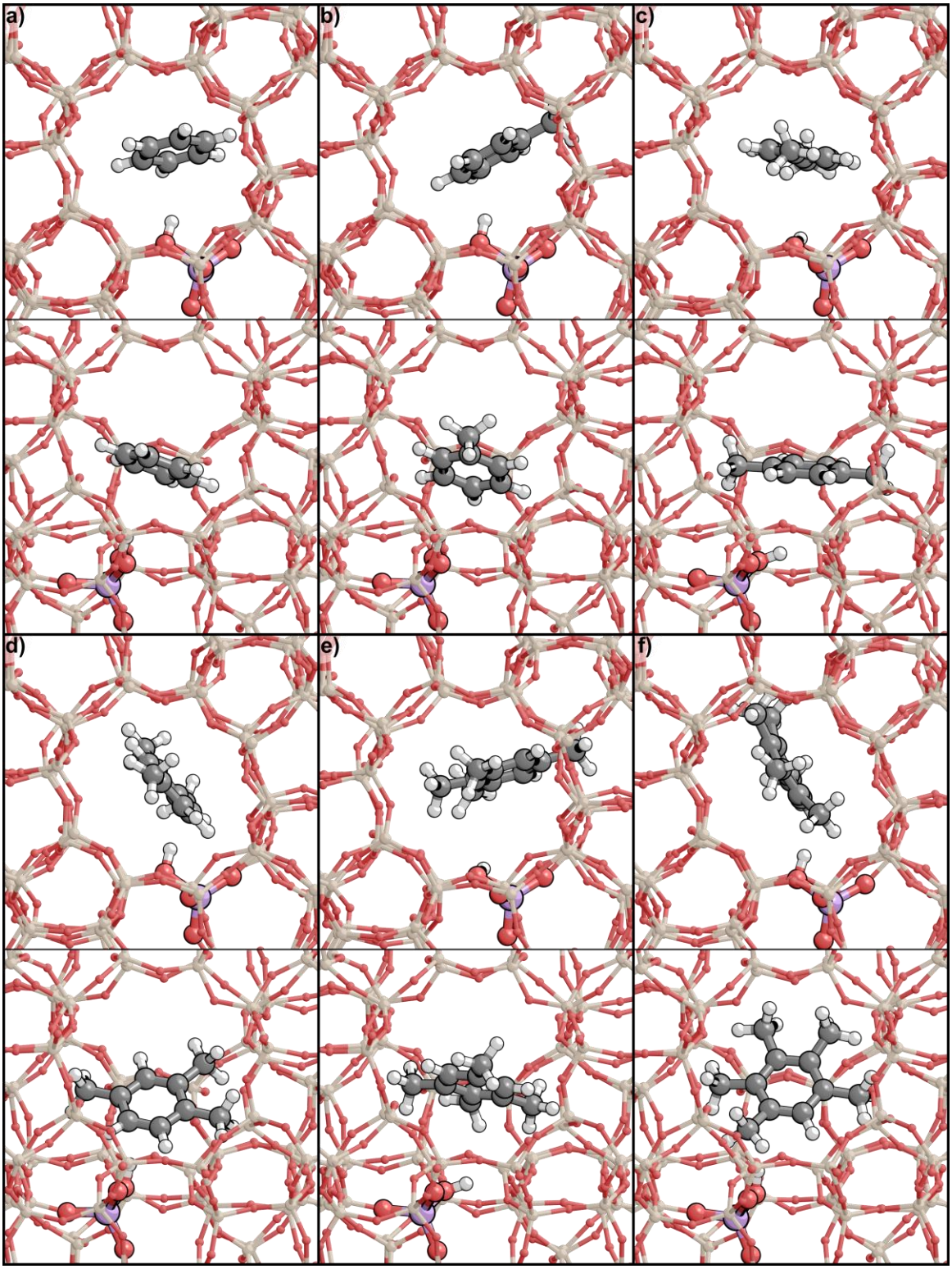

Figure S22. Most favorable orientations of a) benzene, b) toluene, c) *para*-xylene, d) 1,2,4-trimethylbenzene, e) 1,2,3,5-tetramethylbenzene, and f) pentamethylbenzene. Views are shown down the straight channel (top) and sinusoidal channel (bottom)

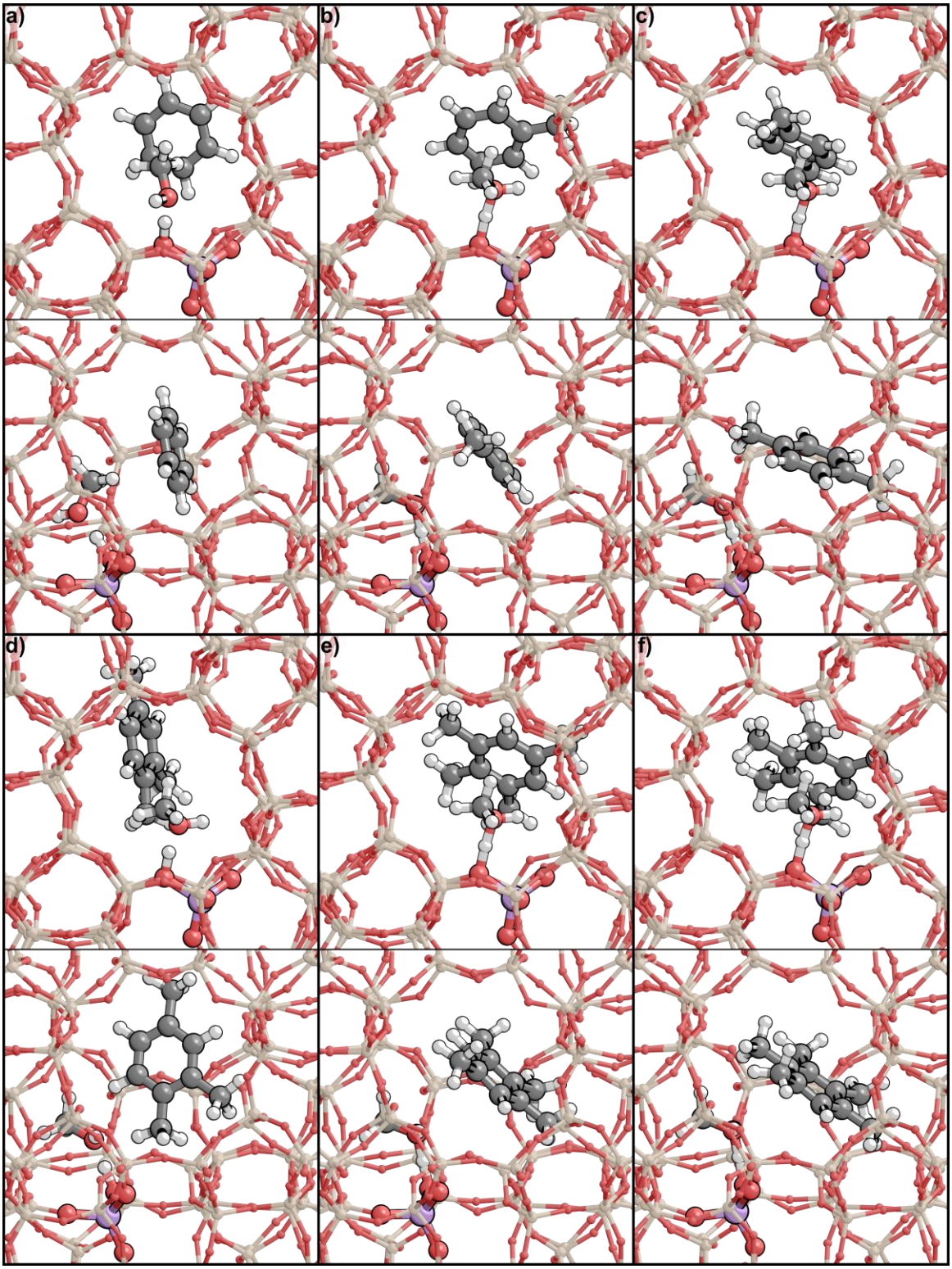

Figure S23. Most favorable orientation of CH_3OH co-adsorbed with a) benzene, b) toluene, c) *para*-xylene, d) 1,2,4-trimethylbenzene, e) 1,2,3,5-tetramethylbenzene, and f) pentamethylbenzene. Views are shown down the straight (top) and sinusoidal (bottom) channels of MFI.

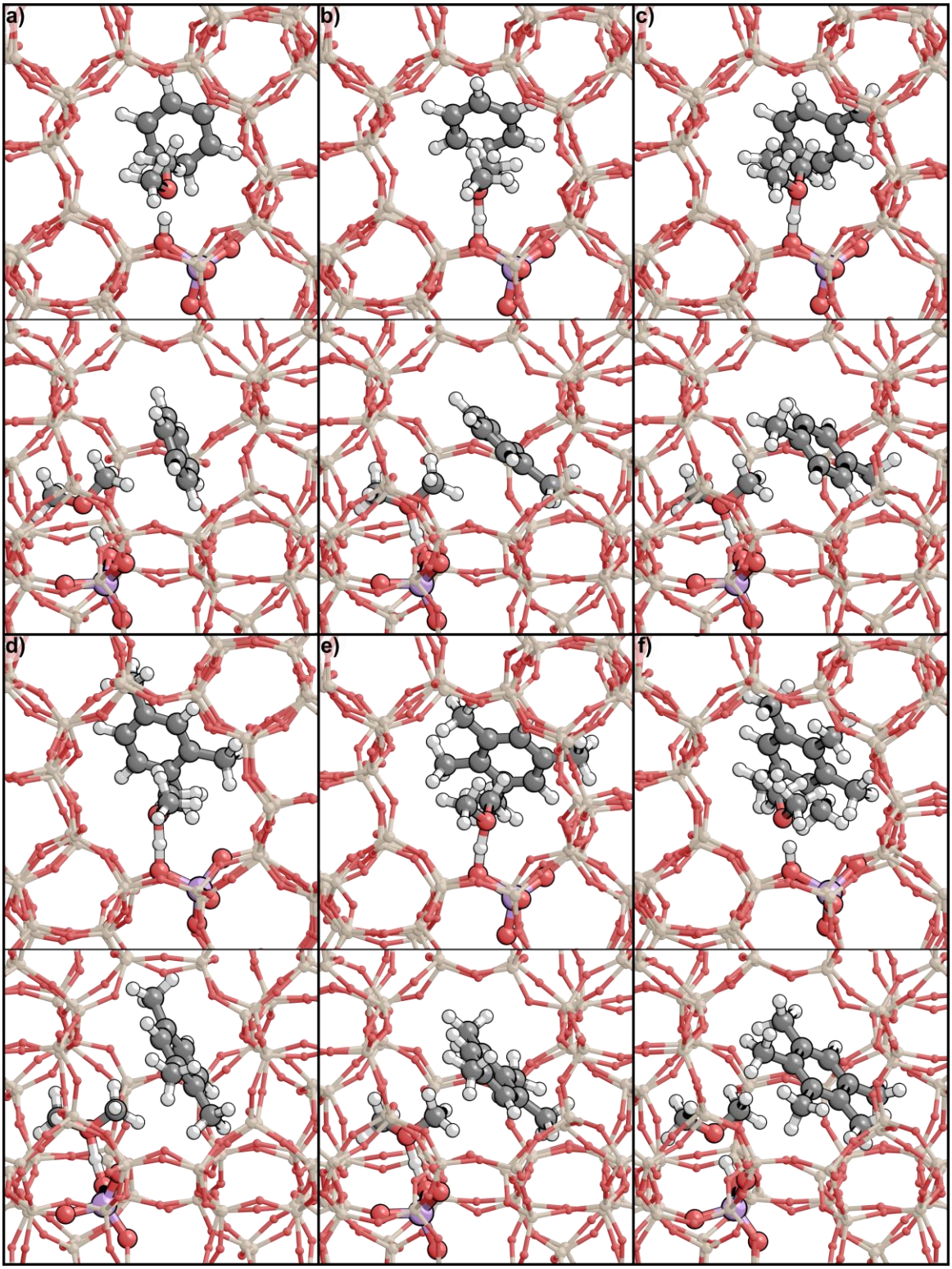

Figure S24. Most favorable orientation of CH_3OCH_3 co-adsorbed with a) benzene, b) toluene, c) *para*-xylene, d) 1,2,4-trimethylbenzene, e) 1,2,3,5-tetramethylbenzene, and f) pentamethylbenzene. Views are shown down the straight (top) and sinusoidal (bottom) channels of MFI.

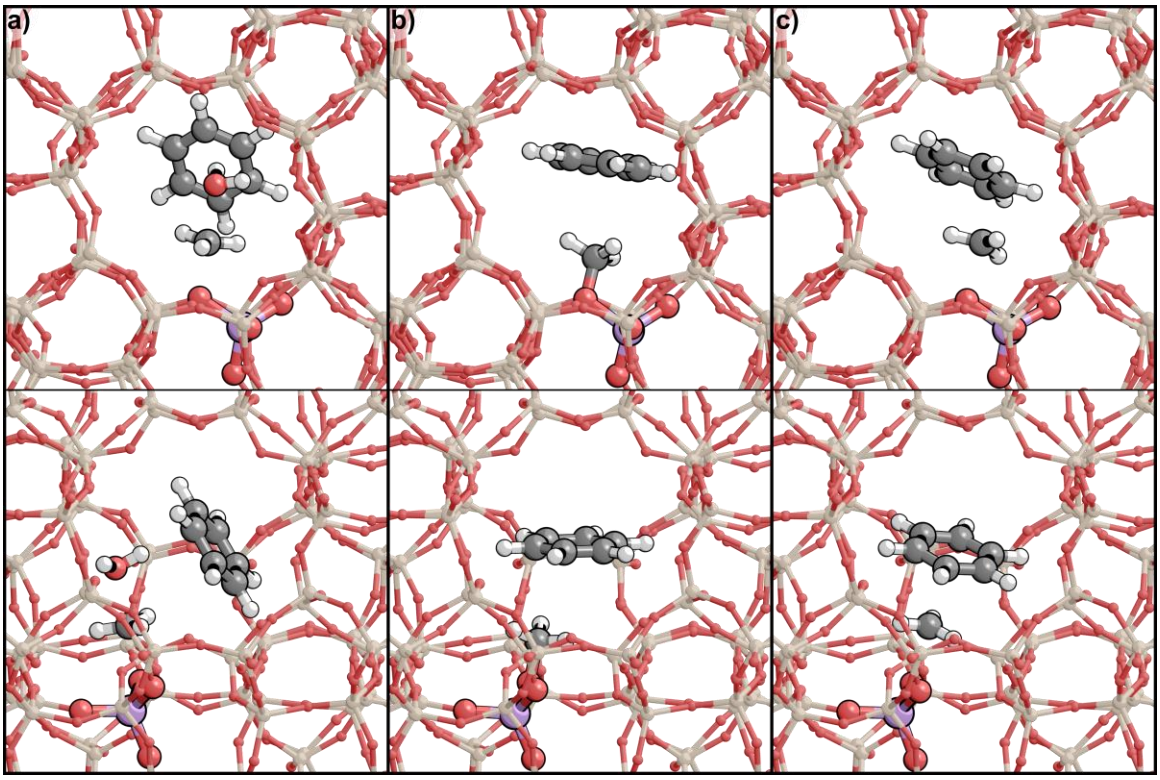

Figure S25. A) Surface methylation, b) CH_3–Z--C_6H_6, and c) ring methylation states of sequential methylation of benzene to toluene by CH_3OH. Views are shown down the straight (top) and sinusoidal (bottom) channels.

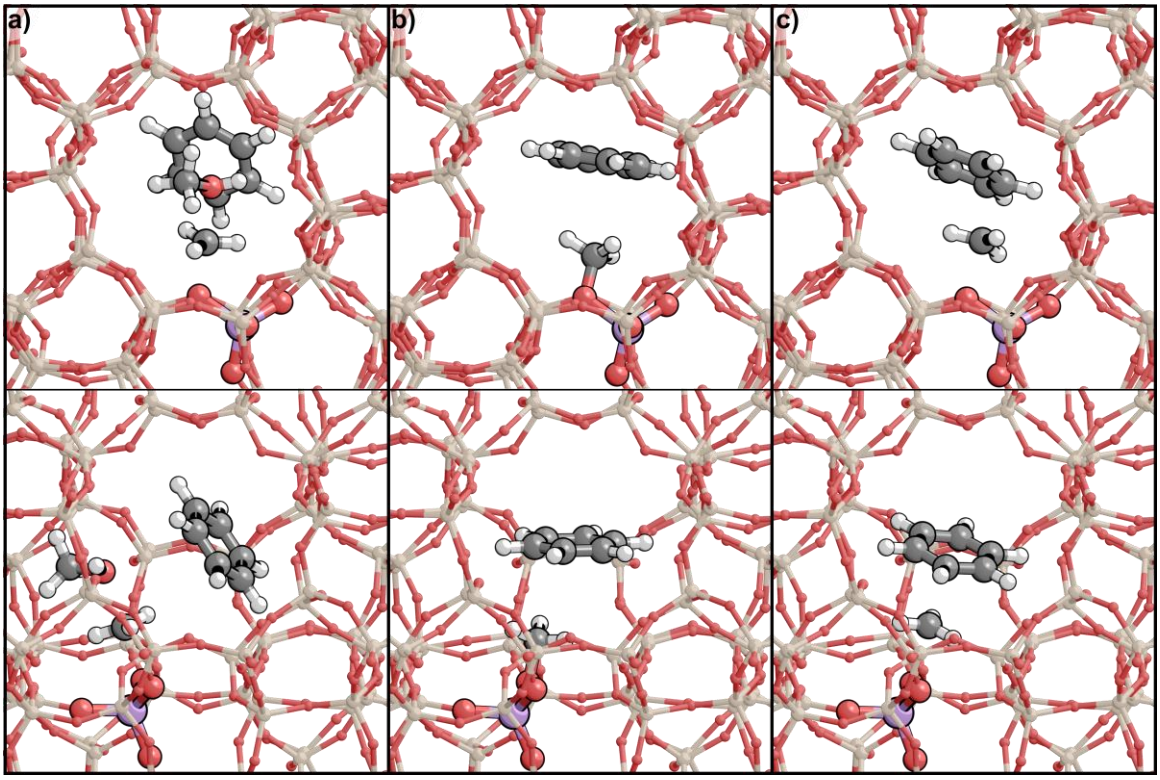

Figure S26. A) Surface methylation, b) CH_3–Z--C_6H_6, and c) ring methylation states of sequential methylation of benzene to toluene by CH_3OCH_3. Views are shown down the straight (top) and sinusoidal (bottom) channels.

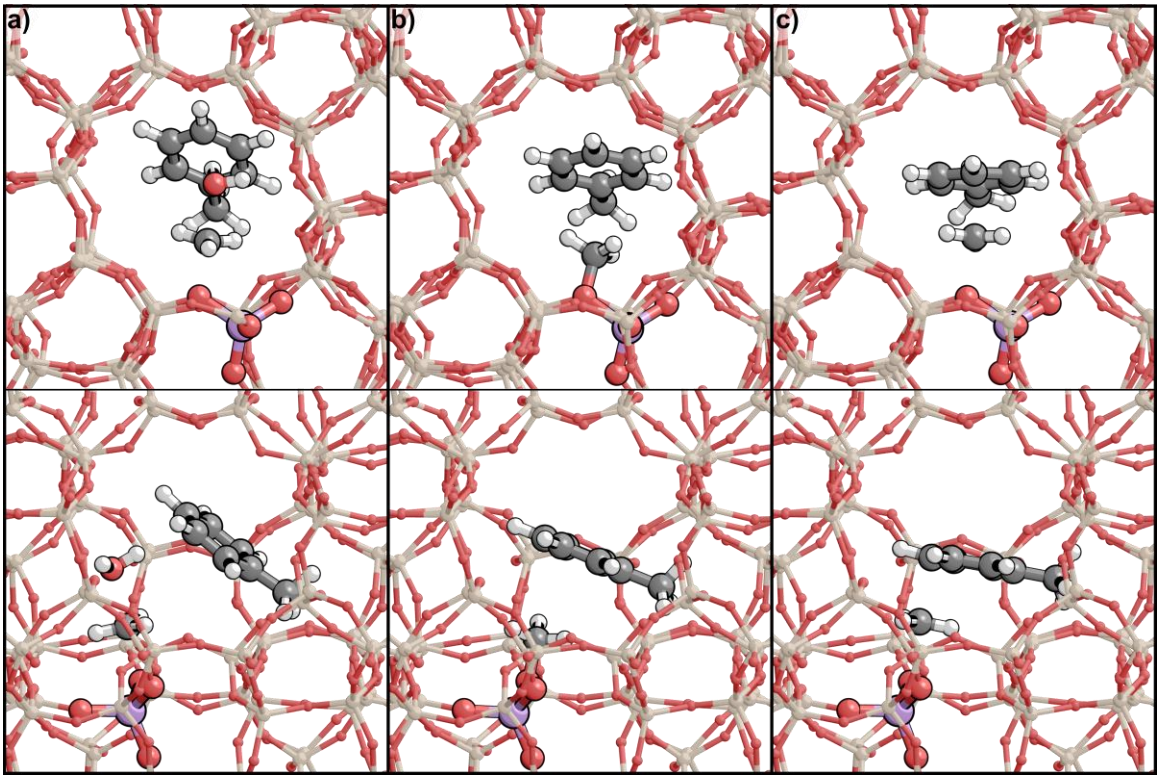

Figure S27. A) Surface methylation, b) CH_3–Z--C_7H_8, and c) ring methylation states of sequential methylation of toluene to *para*-xylene by CH_3OH. Views are shown down the straight (top) and sinusoidal (bottom) channels.

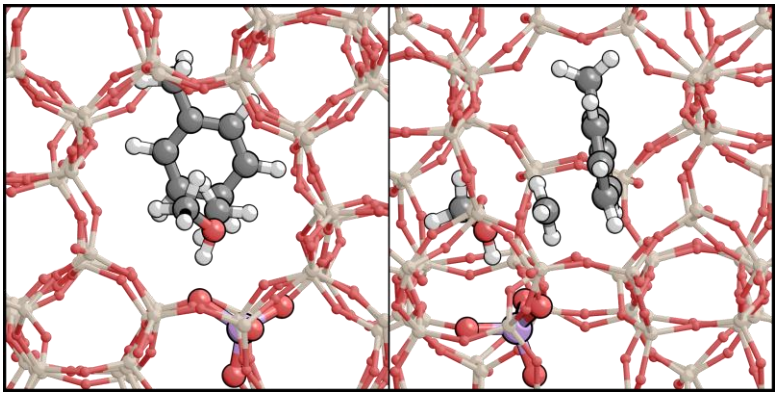

Figure S28. Concerted methylation transition state of toluene into *para*-xylene with CH_3OCH_3. Views are shown down the straight (left) and sinusoidal (right) channels.

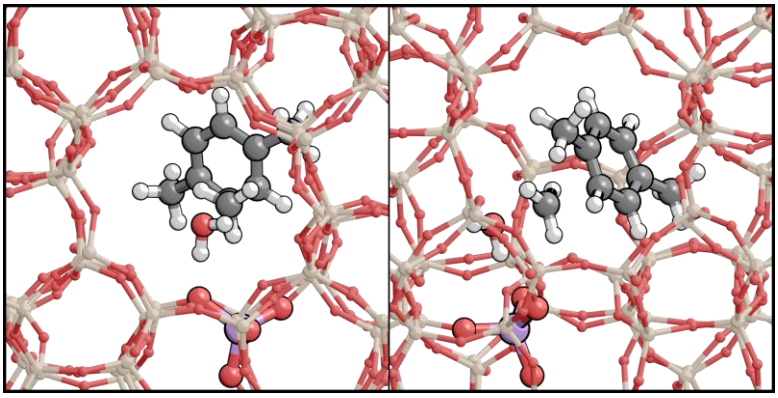

Figure S29. Concerted methylation transition state of *para*-xylene to 1,2,4-trimethylbenzene with CH_3OH. Views are shown down the straight (left) and sinusoidal (right) channels.

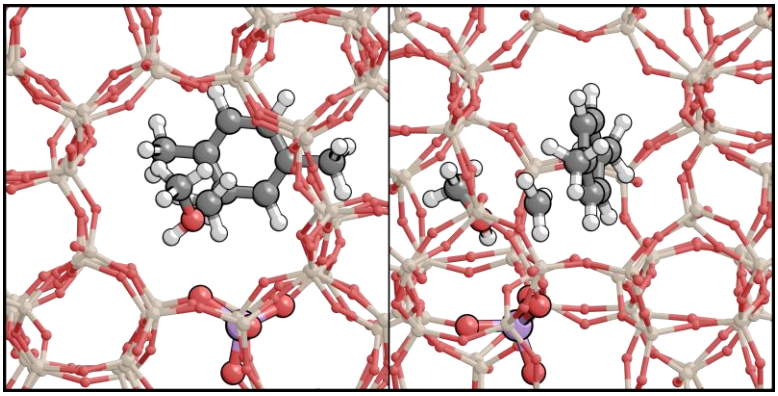

Figure S30. Concerted methylation transition state of *para*-xylene to 1,2,4-trimethylbenzene with CH_3OCH_3. Views are shown down the straight (left) and sinusoidal (right) channels.

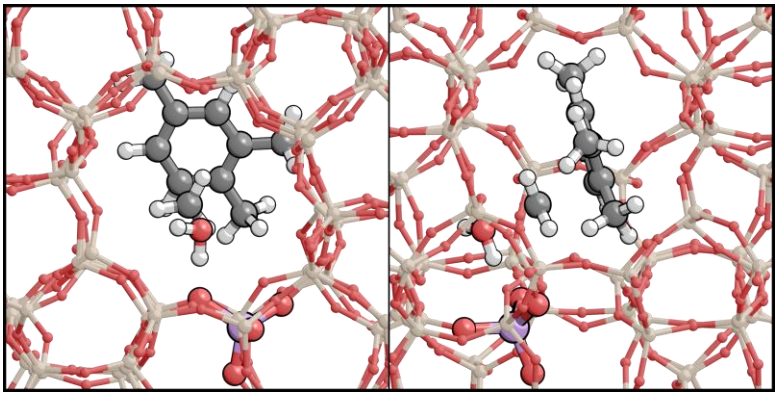

Figure S31. Concerted methylation transition state of 1,2,4-trimethylbenzene to 1,2,3,5-tetramethylbenzene with CH_3OH. Views are shown down the straight (left) and sinusoidal (right) channels.

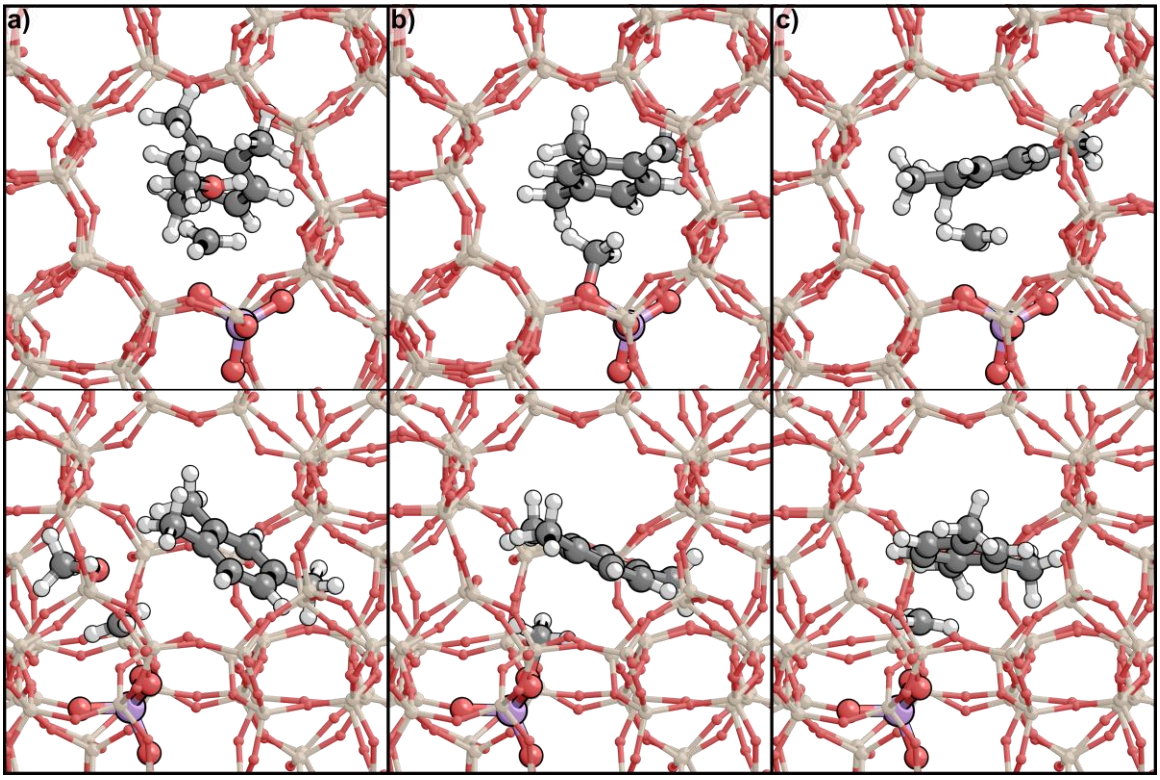

Figure S32. A) Surface methylation, b) CH_3–Z--C_9H_{11}, and c) ring methylation states of sequential methylation of 1,2,4-trimethylbenzene to 1,2,3,5-tetramethylbenzene by CH_3OCH_3. Views are shown down the straight (top) and sinusoidal (bottom) channels.

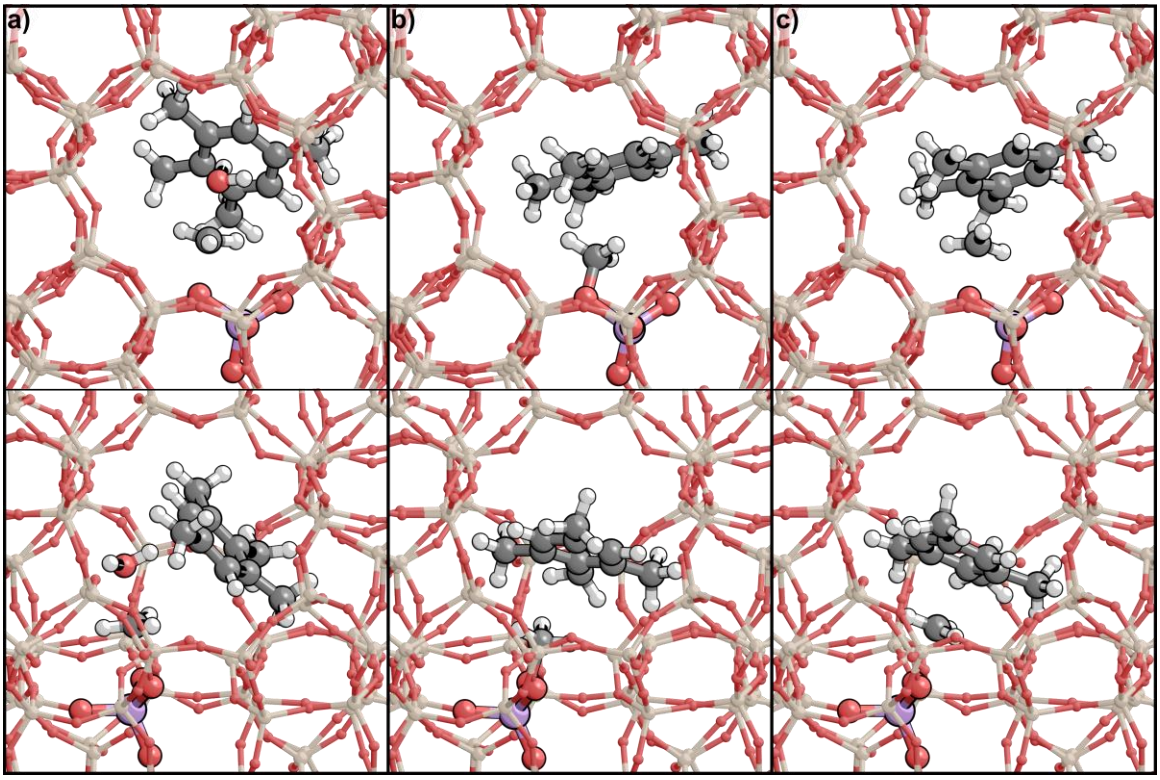

Figure S33. A) Surface methylation, b) CH_3–Z--$C_{10}H_{14}$, and c) ring methylation states of sequential methylation of 1,2,3,5-tetramethylbenzene to pentamethylbenzene by CH_3OH. Views are shown down the straight (top) and sinusoidal (bottom) channels.

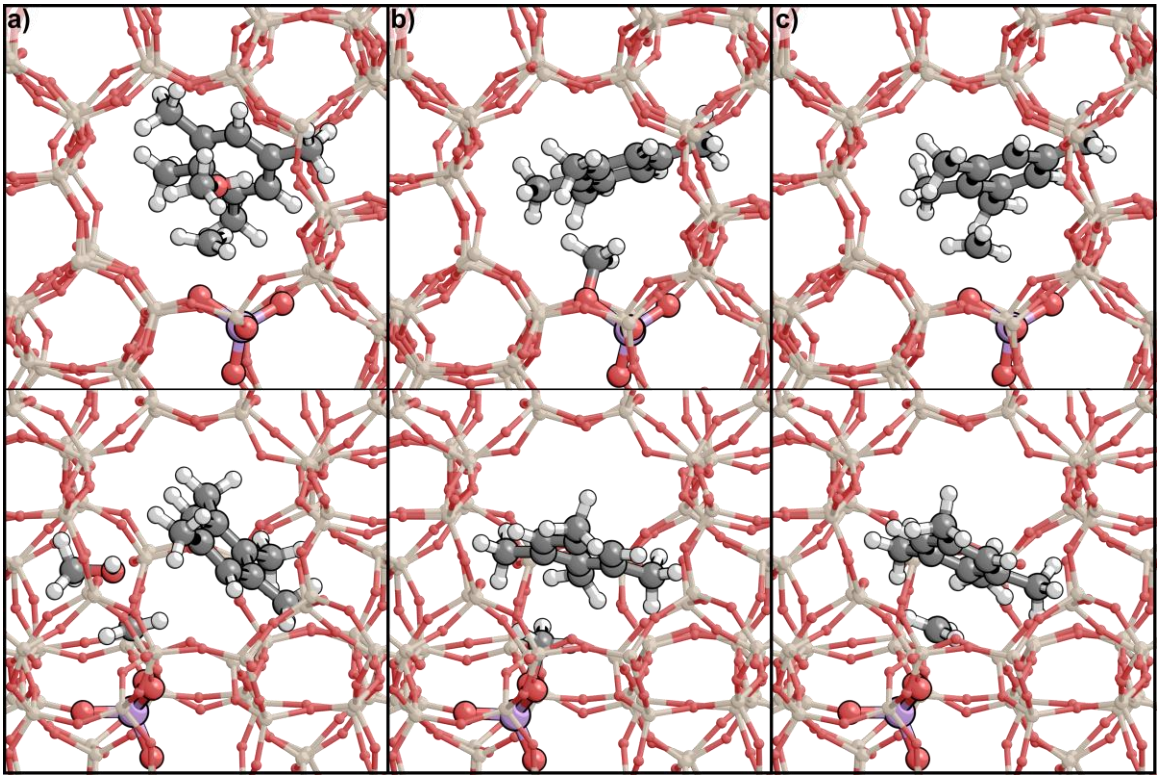

Figure S34. A) Surface methylation, b) CH_3–Z--$C_{10}H_{14}$, and c) ring methylation states of sequential methylation of 1,2,3,5-tetramethylbenzene to pentamethylbenzene by CH_3OCH_3. Views are shown down the straight (top) and sinusoidal (bottom) channels.

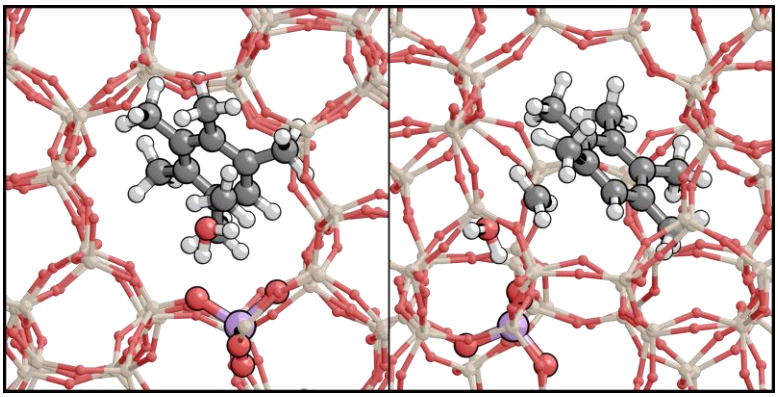

Figure S35. Concerted methylation transition state of pentamethylbenzene to hexamethylbenzene with CH_3OH. Views are shown down the straight (left) and sinusoidal (right) channels.

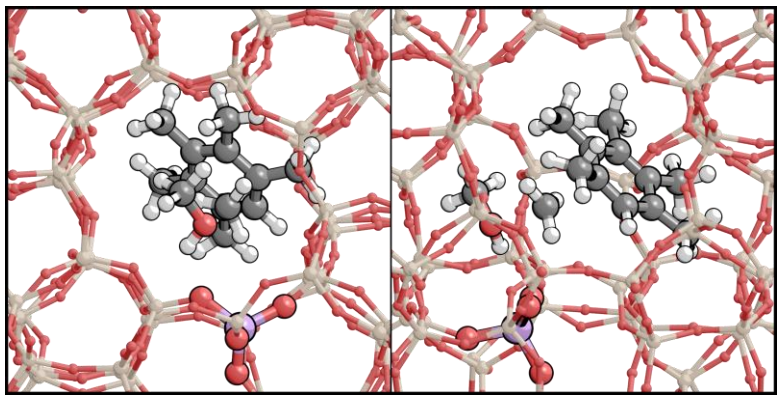

Figure S36. Concerted methylation transition state of pentamethylbenzene to hexamethylbenzene with CH_3OCH_3. Views are shown down the straight (left) and sinusoidal (right) channels.